

Loma Linda University

TheScholarsRepository@LLU: Digital Archive of Research, Scholarship & Creative Works

Loma Linda University Electronic Theses, Dissertations & Projects

6-1983

Development of a Mathematical Model of Renal Function for Clinical Application

Barbara A. Holshouser

Follow this and additional works at: <https://scholarsrepository.llu.edu/etd>



Part of the [Medical Biomathematics and Biometrics Commons](#), and the [Medical Physiology Commons](#)

Recommended Citation

Holshouser, Barbara A., "Development of a Mathematical Model of Renal Function for Clinical Application" (1983). *Loma Linda University Electronic Theses, Dissertations & Projects*. 1002.
<https://scholarsrepository.llu.edu/etd/1002>

This Dissertation is brought to you for free and open access by TheScholarsRepository@LLU: Digital Archive of Research, Scholarship & Creative Works. It has been accepted for inclusion in Loma Linda University Electronic Theses, Dissertations & Projects by an authorized administrator of TheScholarsRepository@LLU: Digital Archive of Research, Scholarship & Creative Works. For more information, please contact scholarsrepository@llu.edu.

Abstract

DEVELOPMENT OF A MATHEMATICAL MODEL OF RENAL FUNCTION FOR CLINICAL APPLICATION

by

Barbara A. Holshouser

This model describes the orthoiodohippurate (OIH) distribution and clearance in the renovascular system. The model is described by five compartments: the blood, left and right kidneys, bladder and the red blood cell compartment. Data for these compartments, except the RBC compartment, are collected with scintillation detectors monitoring OIH tagged with I-131 as the radiopharmaceutical passes through each compartment. Time/ activity curves are plotted for the data and used as inputs to the model parameter estimation routine. The compartments are described by a set of first order ordinary differential equations solved using the Adam's methods. For parameter estimation, an iterative predictor-corrector procedure is used. The estimated model parameters are used to calculate total and differential effective renal plasma flows which are compared to standard PAH clearance tests. A blood-to-urine flow index, defined in this research using these parameters, and a cortex-to-medulla transit is also used to evaluate various renal diseases surgically induced in animal models. The predicted effective renal

plasma flows correlate well with the PAH clearances for both normal and abnormal conditions and the blood-to-urine flow index is particularly useful in differentiating between ureteral obstruction and renal vein occlusion.

UNIVERSITY LIBRARY
LOMA LINDA, CALIFORNIA

LOMA LINDA UNIVERSITY
Graduate School

DEVELOPMENT OF A MATHEMATICAL
MODEL OF RENAL FUNCTION
FOR CLINICAL APPLICATION

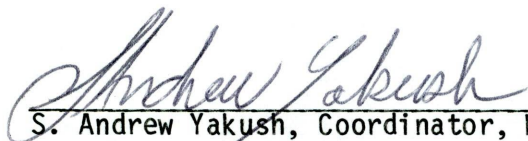
by


Barbara A. Holshouser

A Dissertation in Partial Fulfillment
of the Requirements for the Degree Doctor of Philosophy
in Mathematical Science

June 1983

Each person whose signature appears below certifies that this dissertation in his opinion is adequate, in scope and quality, as a dissertation for the degree Doctor of Philosophy.

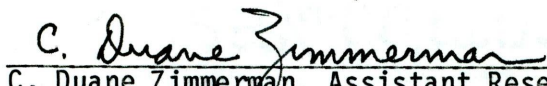

_____, Chairman
S. Andrew Yakush, Coordinator, Mathematical Science Program
Assistant Research Professor in Physiology



George M. Grames, Professor, Nephrology Section,
School of Medicine



Gerald A. Kirk, Associate Professor, School of Medicine



C. Duane Zimmerman, Assistant Research Professor in
Physiology

PREFACE

The purpose of the mathematical model presented in this dissertation is to describe and/or quantitate some aspects of renal function. In the future, we hope to use this model clinically in the nuclear medicine laboratory to aid physicians in diagnosing and evaluating renal diseases in patients.

In Chapter 1, this dissertation summarizes previous work done in this area. Chapter 2 describes the five compartment renal model used in this research and the solution of the equations representing the model. Chapter 3 presents the protocol used for the animal experiments, the results and a discussion of the results. Chapter 4 summarizes and draws conclusions, as well as, states the extensions of this research for future work.

Many people were involved in completing this research and thanks must go to all of them. In particular, thanks go to Dr. Kirk for many hours of catheterizations and to Dr. Grames for much needed advice and evaluation of the data. Thanks must also go to Dr. Yakush and Dr. Zimmerman for help in de-bugging computer programs and special thanks for their encouragement.

TABLE OF CONTENTS

LIST OF TABLES vi

LIST OF FIGURES vii

CHAPTER 1: RENAL SYSTEM: ANATOMICAL AND PHYSIOLOGICAL
SUMMARY AND REVIEW OF PREVIOUS RADIONUCLIDE STUDIES

 Renal Anatomy and Physiology 1

 Filtration, Reabsorption and Secretion 3

 Clearance Concept 5

 Radionuclide Studies 8

 Urinary clearance techniques, single injection
 techniques, single injection techniques using
 external in-vivo counting

CHAPTER 2: MATHEMATICAL MODEL OF RENAL SYSTEM

 Description of Model 17

 Solution of Equations 20

 Inputs to the Model 21

CHAPTER 3: ANIMAL EXPERIMENTS: TESTING THE MATHEMATICAL
MODEL

 Design of Experiments 25

 Experimental Protocol 26

 Surgical protocol, radionuclide studies

 Computer Printout of Model Parameter Estimation
 Routine 33

 Results and Discussion of Parameter Estimates 36

 Results and Discussion of Predicted Effective
 Renal Plasma Flow Estimates 38

Results and Discussion of Blood to Urine
Flow Index 48

Results and Discussion of the Cortex-to-Medulla
Transit Time 50

CHAPTER 4: SUMMARY AND CONCLUSIONS

Summary 54

Conclusions 55

REFERENCES 57

LIST OF TABLES

TABLE		PAGE
1	Estimated Model Parameters	37
2	PAH Clearances Compared to Predicted ERPF's	39
3	Inulin Clearances (GFR)	40
4	Left and Right Kidney Blood-to-Urine Flow Indexes	49
5	Left and Right Kidney Cortex-to-Medulla Transit Times	52

LIST OF FIGURES

FIGURE		PAGE
1	Diagram of Basic Anatomical Features of the Urinary System	2
2	Diagram Comparing the Anatomy of Nephrons	4
3	Diagram of the Three Basic Process of Urine Formation	6
4	Diagram Representing a Five Compartment Model of the Mammalian Renal System	19
5	Summed Images of Kidneys and Flagged Regions of Interest	30
6	Time/Activity Curves Obtained From Scintillation Detectors for Normal and Abnormal Studies	31
7	Color Coded Phase Images of Normal and Abnormal Studies	32
8	Computer Printout of Compartment Model Identification Program	34

CHAPTER 1

RENAL SYSTEM: ANATOMICAL AND PHYSIOLOGICAL SUMMARY AND REVIEW OF PREVIOUS RADIONUCLIDE STUDIES

Renal Anatomy and Physiology

The kidneys are paired organs which constitute on the average 0.4% of the weight of the body, yet, at rest, renal blood flow amounts to 20-25% of cardiac output(40). The high blood flow to the kidneys is related to the several vital functions the kidneys perform for the body. Not only do the kidneys eliminate metabolic waste products, they also regulate fluid balance and electrolytes such as sodium and potassium and perform some endocrine functions. Figure 1 illustrates some of the basic anatomical features of the urinary system, including the distinction between the outer portion of the kidney, called the cortex, and the inner portion, called the medulla.

To perform its functions, each kidney is composed of approximately one million units called nephrons each of which are capable of producing urine(28). Each nephron is composed of a glomerulus which filters plasma and a tubular portion which functions not only as a conduit but, also is responsible for ultimate regulation of fluid and electrolytes.

The anatomy of the nephron is described by following the path of the fluid flow through the kidney. Blood enters the kidney in the renal artery which branches into a series of successively smaller arteries and finally into afferent arterioles each of which leads into the glomerulus of a nephron. The capillaries of the glomerulus are suspended in the ultrafiltrate in Bowman's capsule. Since the net pressure in the

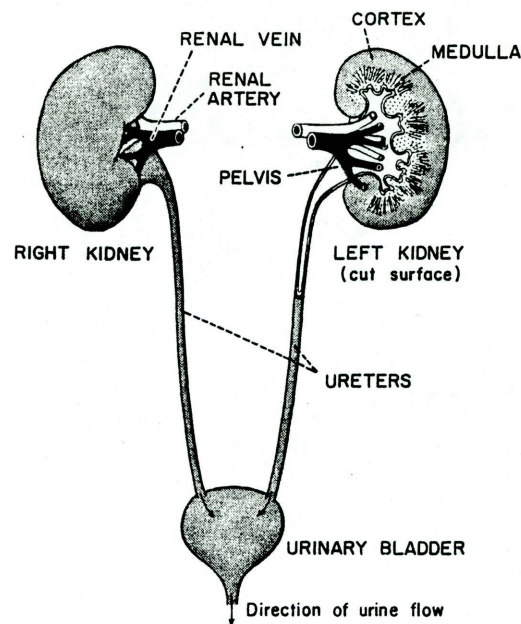


Figure 1. The basic anatomical features of the urinary system from Guyton(28).

capillaries of the glomerulus is higher than the pressure of the ultrafiltrate in Bowman's capsule(2), plasma water is filtered through the capillary membrane. The epithelium of Bowman's capsule is continuous with the proximal tubule. Ultrafiltrate from Bowman's capsule first enters the proximal tubule lying in the cortex of the kidney. From there, the fluid continues into a sharp hairpin-like loop called the loop of Henle. Cortical nephrons which make up approximately 85% of all the nephrons(4) have glomeruli which are located in the outer cortex and the descending loop of Henle protrudes only into the outer medulla. The remaining 15% of the nephrons have glomeruli which lie close to the medulla with long thin descending portions of the loop of Henle which descend deep into the medulla. These nephrons are called juxtamedullary

nephrons. The ascending loops of Henle for both types of nephrons continue up into the cortex into the distal tubule. The distal tubules of several nephrons then empty into a collecting tubule or collecting duct. This duct descends into the medulla paralleling the loops of Henle and empties into the renal pelvis. Figure 2 shows the anatomy of cortical and juxtamedullary nephrons.

The afferent arteriole after branching into the network of capillaries of the glomerulus recombine to form the efferent arteriole which leaves Bowman's capsule only to form a second network of capillaries called the peritubular capillaries. Blood perfuses the cortical interstitium around both the proximal and distal tubules in the peritubular capillaries. Efferent arterioles from glomeruli of juxtamedullary nephrons also branch into the medulla. These vessels, called vasa recta, are long and descend parallel with the loops of Henle deeply into the medulla. The vasa recta then loop back up into the cortex and empty into the cortical veins along with the peritubular capillaries. Figure 2 also compares the blood supplies of cortical and juxtamedullary nephrons.

Filtration, Reabsorption and Secretion

The function of nephrons is to form urine and in doing so clear the body of metabolic wastes and regulate sodium, potassium, chloride and hydrogen ions(64). The nephrons use three basic processes to accomplish this: glomerular filtration, tubular reabsorption and tubular secretion.

Blood perfusing the glomerular capillaries is under hydrostatic pressure thereby initiating the formation of urine. Cellular elements, large protein molecules and lipids are prohibited from passing through

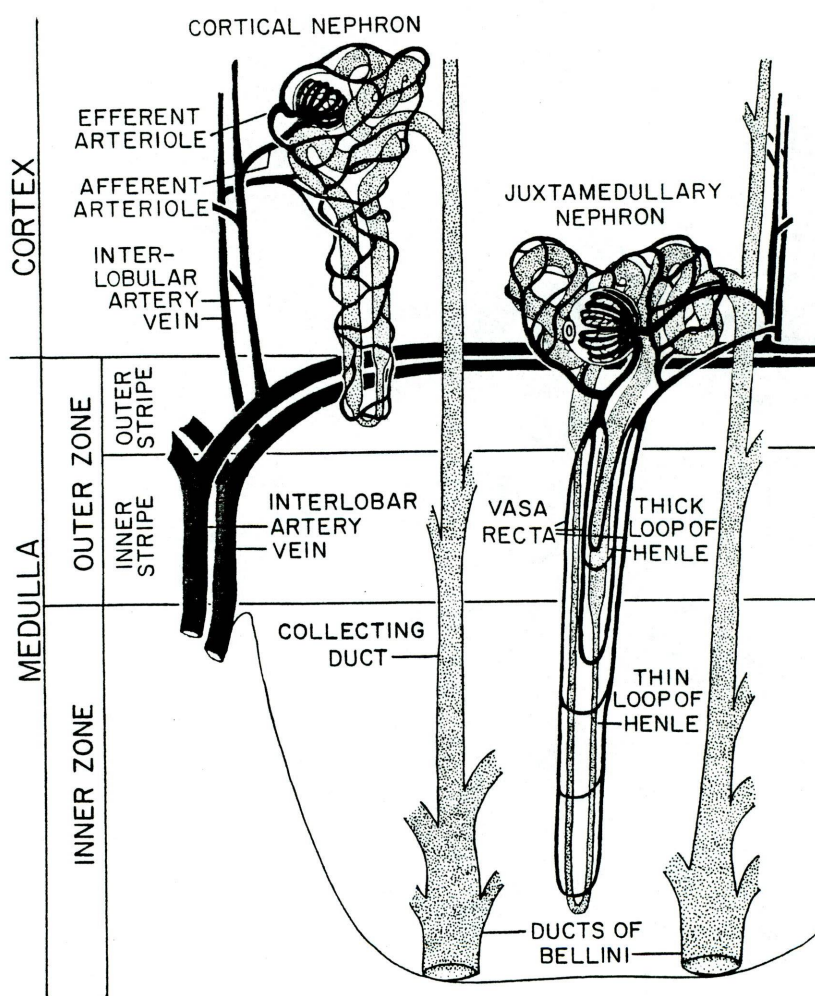


Figure 2. Comparison of the anatomy including the blood supplies of cortical and juxtamedullary nephrons. From Pitts (40).

the capillary membrane due to either their size or charge, so that the ultrafiltrate appearing in Bowman's space is essentially protein and cell free(2). This process is called ultrafiltration. The volume of plasma filtered per unit time is known as the glomerular filtration rate (GFR). Guyton estimates that one-fifth of the plasma that flows through the glomerular capillaries is filtered into Bowman's capsule and enters the tubular portion of the nephron(28). The normal value for the GFR of a

70 kg man is 125 ml/min.

Due to the large portion of plasma filtered through the glomeruli each day, some process must be used to retain extracellular fluid volume and return valuable solutes present in the filtrate to the peritubular capillary fluid. This process is called reabsorption. With average intake, approximately 99% of the salt and water filtered each day is reabsorbed, however, the kidney has tremendous capability to vary this percentage considerably in order to maintain homeostasis. The rate of reabsorption is the difference between the rate of filtration and the rate of excretion. Reabsorption occurs through the tubule walls by both active and passive mechanisms. Solute such as sodium, glucose and phosphate require active transport mechanisms, while urea and water are passively reabsorbed following concentration gradients.

The other process used in urine formation is called tubular secretion. Secretion is used to transport substances into the tubular lumen and may be either active or passive. The rate of secretion is equal to the rate of excretion minus the rate of filtration. Figure 3 illustrates the three basic processes of urine formation.

Clearance Concept

The clearance of a substance is defined as the volume of plasma from which that substance is completely cleared by the kidneys per unit time(65). Plasma clearance varies for different substances and can be calculated by the following basic formula:

$$\text{Plasma (ml/min) clearance} = \frac{\text{Quantity of urine(ml/min)} \times \text{conc. in urine(mg/ml)}}{\text{Concentration in plasma (mg/ml)}} \quad (1)$$

The concept of plasma clearance is important because it can be used

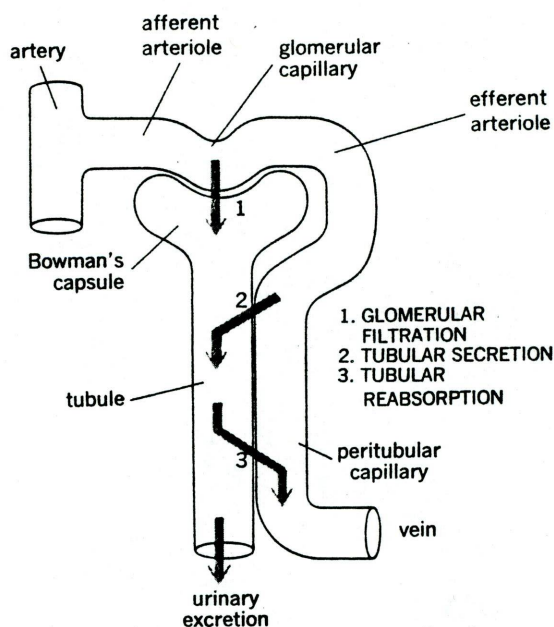


Figure 3. The three basic processes of urine formation. From Vander (64).

to measure different aspects of kidney function.

Inulin clearance is one of the most important clearance measurements made. Inulin is metabolically inert, is not protein bound and is freely filtered at the glomerulus. Since inulin is neither reabsorbed nor secreted by the renal tubules, the amount of inulin excreted in the final urine is equal to the amount filtered by the glomeruli per unit time(2). Therefore, inulin clearance is a measure of glomerular filtration rate (GFR). The clearance of inulin to measure GFR was first proposed by Richards, et al and Shannon and Smith in 1935(4). One drawback to inulin measurement is that inulin does not normally exist in

human plasma and so must be constantly infused to maintain a constant level in the blood in order to perform the clearance measurement. However, creatinine is normally found in human plasma at relatively constant levels(2) and exhibits most of the same properties of inulin except that it is partially secreted (approximately 20%). This tubular secretion of creatinine makes its clearance value proportionately higher than that of inulin. In the human adult male, the average normal value for inulin clearance is 135 ml/min corrected to 1.73 square meters of body surface area, whereas, the average normal creatinine clearance is 164 ml/min corrected(2).

Para-aminohippuric acid (PAH) clearance is another important measurement of renal function. PAH, like inulin, is metabolically inert, is not produced by the body, is freely filtered by the glomerulus and is not reabsorbed by the tubules. Unlike inulin, however, PAH remaining in the plasma after filtration is almost completely secreted by the tubules(41). Since PAH is almost completely cleared by both filtration and secretion in a single pass through the kidneys, PAH clearance may be used as a measure of renal plasma flow. In practice, since the extraction of PAH in the normal adult man is on the average equal to 90%(53), the true renal plasma flow is underestimated by PAH clearance. Therefore, the term, effective renal plasma flow (ERPF) has been used to describe PAH clearance(3). If the extraction ratio for PAH (E_{PAH}) is known, then the true renal plasma flow (RPF) may be calculated as follows(3):

$$RPF = ERPF (ml/min)/E_{PAH} \quad (2)$$

If simultaneous measurement of inulin and PAH is made at low plasma PAH levels, then the fraction of plasma filtered through the glomeruli, known as the filtration fraction, can be calculated using the following equation(41):

$$\text{Filtration Fraction} = C_{\text{IN}}/C_{\text{PAH}} = \text{GFR}/\text{ERPF} \quad (3)$$

In a normal adult man, the filtration fraction is 16-20%(41).

Radionuclide Studies

The clearance studies previously mentioned, utilizing inulin for GFR determination and PAH for determining the ERPF, are not routinely used clinically due to their demanding, invasive nature. The standard urinary clearance technique involves constant intravenous infusion of the substance to be measured and bladder catheterization for collection of urine. This makes the presence of a physician mandatory and the accurate collection of blood and urine samples absolutely important. The use of radioactive tracers substituted for these chemical substances has become a widespread practice. The goal is to increase the ease and accuracy of the analyses, since scintillation counting of a gamma emitting radionuclide is faster and easier than chemical analyses(61).

I-131 or I-123 labeled orthoiodohippurate (OIH) are the most commonly used radiopharmaceuticals for the determination of effective renal plasma flow. I-131 and I-123 are both gamma photon emitting radionuclides with energies of 364 keV and 159 keV respectively. I-125 OIH with gamma photon energies of 28 and 35 keV, has also had limited use. The similarity in renal handling of orthoiodohippurate (OIH) and para-aminohippurate (PAH) was first established in man by H. W. Smith and

co-workers(55). Smith compared clearance ratios of unlabeled OIH, PAH and Diodrast and found these ratios to be within .95 to .97 in both dog and man using urinary clearance techniques developed in his lab.

Realizing the advantages of labeling OIH with a radioactive tag so that external measurements could be taken, Tubis, Posnick and Nordyke in 1960, were first to successfully label OIH with I-131(63). The following year, Mitta et al, simplified Tubis' technique(36).

Urinary Clearance Techniques

Using the urinary clearance techniques of Smith(55), several investigators soon reported using the I-131 labeled OIH to measure effective renal plasma flow. Schwartz and Madelhoff(48,49) performed simultaneous PAH and radio-OIH clearance studies on twenty-five patients in which they found the average C_{OIH}/C_{PAH} clearance ratio to be 0.814. Burbanke and Tauxe(13), working independently, also compared PAH and I-131 OIH in man and reported an average C_{OIH}/C_{PAH} clearance ratio of 0.87. Later, other investigators confirmed these clearance ratios in man(7,47).

Several theories have been suggested to explain why radio-OIH has a lower clearance than PAH. Burbank(13) suggested that the presence of free iodide in the I-131 OIH may cause the failure to achieve the expected ratio of 1.0. However, Meschan et al,(35) reported a low clearance ratio with less than 1% free iodide in the preparation. Magnusson(32) related the discrepancy to the high specific activity of the I-131 OIH, causing autoradiolysis and a higher free iodide content. As a result, in 1967, I-131 was replaced with I-125 with a lower specific activity to tag OIH and higher clearance ratios of 0.90 by Ram et al(43)

and 0.96 by Cutler and Glatte(16) were reported. Much later in 1980, Stadalnick et al(56) tagged OIH to I-123 and reported a lower OIH to PAH clearance ratio of 0.86.

A second theory was postulated to explain why I-131 OIH has a lower clearance than PAH. Since OIH is bound to protein by as much as 50% more than PAH, Schwartz and Medelhoff(49) suggested that the protein binding retards diffusion from the peritubular capillaries to the interstitial fluid. Summers et al(58) used protein-free plasma filtrates to calculate the I-131 OIH/PAH clearance ratio in dogs and reported 0.96. Additionally, by administering stable iodohippurate to take up the binding sites, Summers reported a clearance ratio of 0.97. Maher and Tauxe(33) used plasma filtrates in man and reported a clearance ratio of 0.92.

Later, Gagnon et al(25), concluded from his studies that the presence of PAH alters the clearance of I-131 OIH by inhibiting tubular secretion. This finding accounts for only part of the discrepancy between the clearance ratios of I-131 OIH and PAH during simultaneous measurements, so that, free iodide or protein binding may account for the remaining discrepancy.

Single Injection Techniques

In 1956, Taplin and co-workers(60) first introduced the "radioisotope renogram" which involved a single intravenous injection of a radioiodinated substance followed by a continuous recording of the radioactivity in the renal area. This led other investigators to develop a method of determining ERPF utilizing the single injection technique. This method obviated the necessity for constant infusion and bladder

catheterizations used in the chemical analysis technique of determining ERPF. The single injection method is based on the assumption that the function being measured will clear the substance after injection into the blood and, therefore, the clearance rate becomes a measure of the function(61). Quantitative estimates of renal function are then possible, by the application of parameter estimation techniques to compartmental models of the renal system, yielding information not obtainable from the conventional renogram.

Early investigators compared the clearance ratios of I-131 OIH to PAH. I-131 OIH was first measured by using a scintillation well counter to count the levels of I-131 in blood or plasma samples taken serially after a single injection while simultaneously measuring PAH clearances by the standard urinary clearance technique. Gott and co-workers(27) using a one compartment model to analyze plasma curves, reported excellent correlation ($I-131\ OIH/PAH = 1.01$) with PAH clearances in man. With a one-compartment model, Gott assumed that after a single injection, OIH came to equilibrium in the blood within minutes and was then cleared from the single blood compartment only by the kidneys. Dabaj and Pritchard et al(17) extended Gott's work using the one compartment model to find that renal blood flow determined by single injection of I-131 OIH to be within 7.6% of direct measurements of flow in dogs. The same group of investigators later found the correlation of single injection to PAH clearances to be within 5.6% in humans(42).

Blaufox et al, interpreted the disappearance of I-131 OIH from plasma in dogs(10) following the two compartment system of Saparstein(45) and a three compartment system. The model predictions for the cardiac

and renal curves were compared to actual data obtained by external counting with NaI scintillation probes. Blaurox found that both models were successful in predicting I-131 OIH clearance after single injection and therefore recommended and later used the simpler two-compartment system for analysis of renograms in man(7,9). The two compartment model consisted of a blood (heart) compartment and renal (kidneys) compartment and assumed only that the OIH in the renal compartment is freely available to the plasma.

Other investigators also used a two compartment model to interpret curves of I-131 OIH disappearance in blood to measure effective renal plasma flow. Wagoner, Tauxe and Maher(67) using the two-compartment model, reported that the ERPF found by the single injection technique was an average of 5% less than the standard PAH clearance found in man. The same group, Tauxe et al, modified their studies to evaluate compartmental analysis for the simultaneous determination of ERPF and GFR using two different radiopharmaceuticals(24). Later, Tauxe et al, simplified their method of measuring ERPF so that only one plasma sample must be taken after a single injection of I-131 OIH(62), however, this method seemed to result in loss of accuracy.

Equations for a three-compartment model, first proposed by Matthews(34), in which the urine (bladder) compartment is included, were used by Chisholm and co-workers to calculate ERPF using the clearance of I-125 OIH by analyzing blood samples from dogs in a scintillation well counter(14). These results were also compared with renal blood flow measurements directly made in dogs and were found to correlate well.

Single Injection Techniques using External In-Vivo Counting

Witcofski et al, using two matched scintillation detector probes positioned over each kidney was first to propose that external counting of I-131 OIH over the kidneys ("the renogram") could be analyzed to provide a measure of renal function(69). Later, Taplin, Dore and Johnson, extending Witcofski's work, reported methods to determine total and differential renal blood flow in man(59).

In 1967, Blaufox and co-workers(11) also reported a method to measure ERPF in man by external counting. However, one scintillation probe placed over the head was used to count I-131 OIH in the blood after a single injection instead of counting over the kidney. The curve resulting from the continuous counts over the head was used in a two compartment model to calculate ERPF which was correlated with PAH clearances ($r=0.89$).

A similar single injection technique in man was used by Ram, Evans and Chisholm(44) utilizing a single compartment model and external counting of I-125 OIH in the blood over the heart. Their results showed that although the correlation with standard PAH clearances were satisfactory, the absolute values differed. This difference was attributed to background activity.

In 1969, Holroyd et al, suggested using the gamma camera for obtaining dynamic quantitative information from renogram curves by storing data from the gamma camera on magnetic tape for analysis(29,30). There are several advantages of using the gamma camera instead of probes for obtaining renogram curves, one of which is the elimination of errors associated with probe positioning since the field of view of the standard

gamma camera is twelve inches in diameter. A second important advantage is related to the physical performance of the gamma camera. The sensitivity of the gamma camera is almost constant in a plane at right angles to the camera axis and decreases more slowly than the sensitivity of a probe, as the distance from the face of the camera increases. Since the kidneys are posterior organs, when posterior views are taken, the distance from the face of the camera is small, so that the sensitivity and resolution are nearly equal for each kidney. Another advantage of the gamma camera is that due to the fact that two dimensional sequential images are obtained during the renogram, data on the intrarenal transport of OIH can be obtained which is impossible with an ordinary probe.

The following is a review of the literature in which renal function is evaluated by external counting using gamma cameras.

Schlegel and Bakule used sequential renal scintillation scan data recorded on magnetic tape to estimate individual renal function. They found a high qualitative correlation with comparative information obtained from excretory urography, biopsy and necropsy(46).

Using a modification of Schlegel's work Hayes, Brosman and Taplin(31) determined split renal function in dogs using sequential renal scintigraphy also recorded on magnetic tape. This method was based on quantitation of three areas of interest (left kidney, right kidney and pelvic background) during the one to two minute post-injection period of I-131 OIH. The advantage of selecting areas of interest, as recommended by Farmelant(23), is to exclude unwanted peripheral background activity. The percentage of total renal function for each kidney was calculated and correlated well ($r = 0.974$) with the standard constant infusion OIH

clearance using individual urine collection techniques. Complicated models or computers were not used in this method since only simple ratios were calculated, however, absolute values of ERPF were not found.

Chisholm et al(15,51) described a method of measuring differential renal plasma flows in man using I-123 OIH, the gamma camera and a digital computer. A region of interest from the gamma camera images located centrally and just above the kidneys was used to calculate ERPF by their single compartment model. This value was compared to PAH determinations indirectly, by using a heart probe to count I-125 OIH after a single injection technique previously described. A correlation coefficient of 0.963 was calculated for the two sets of data showing that the gamma camera can be used to accurately assess ERPF. Tubular transit time was estimated using regions of interest for the cortical and medullary regions from the gamma camera images of the kidneys. The computer was used in this study to flag the regions of interest and subtract a normalized background region from them, as described by Britton and Brown(12) earlier.

A few years later, a more complicated approach was reported by DeGrazia et al(19) using a seven compartment model that considered the distribution and rates of exchange of I-131 OIH into red cells, plasma and extravascular compartments, as well as, the tubular cells of the kidney. Measurements of individual ERPF, urine flow fraction and tubular transport time were reported in forty nine patients with normal and abnormal renal function and compared these values with conventional split-function techniques using PAH and inulin. This technique used a gamma camera electronically split for counting the kidneys and two

scintillation probes recording counts from the heart and bladder. The data recorded were transmitted by a teletypewriter over telephone lines to a computer for processing. The following assumptions were made for the computations. After injection of OIH, it is distributed between free OIH in plasma, the red cells, plasma proteins, interstitial and extracellular spaces. Exchange of OIH between the free and bound state is assumed to be rapid; glomerular flow is small; reabsorption does not take place; and OIH is cleared before it is efferent to the proximal tubular cells.

In DeGrazia's work, no regions of interest were flagged since only counts from the probes and each half of the gamma camera could be transmitted to the computer. As a result, elaborate mathematics to correct for "crossover" counts between kidneys were included in the parameter estimations. In addition, although no specific regions for medullary and cortical areas of the kidneys could be flagged, rate coefficients for the flow of OIH from the tubular cells into the tubular lumen of each kidney was reported. Tubular transport time, defined by DeGrazia as the time delay between tubular cell outflow and renal pelvic outflow, was also reported for each kidney.

DeGrazia's procedure was used clinically in Loma Linda's Nuclear Radiology department and was found to be unsatisfactory due to obvious inaccuracies for some patients. It was at this time that we decided to develop our own model to calculate various parameters of renal function to replace this procedure in the clinical laboratory. The following chapters are a report of this research.

CHAPTER 2

MATHEMATICAL MODEL OF THE RENAL SYSTEM

Description of Model

This model describes the OIH distribution and clearance in the renovascular system. At this time, it is necessary to consider the assumptions made in setting up the mathematical model. The assumptions made are the following: a) it is assumed that after introduction into the blood stream, OIH is distributed through plasma and red blood cells within the first minute after injection(19). OIH, unlike PAH, diffuses into the red blood cells which this model takes into account. Burbank et al(13) reported 29% binding to red blood cells and Magnusson(32) reported an average of 33% binding. Magnusson also reported no binding of OIH to plasma proteins(32). It is also assumed that mixing through the blood compartment is extremely rapid in relation to removal from this compartment. b) It is assumed that OIH is neither destroyed nor produced in the body(13). c) It is assumed that OIH is cleared by the kidneys and not reabsorbed. d) It is assumed that the rate constants are proportional to the quantity of tracer material in the anatomic pool. Specifically, it is assumed that the rate of uptake by the renal parenchyma is proportional to the blood concentration of I-131 OIH. We feel this may be assumed since the concentration of I-131 OIH is kept low and the transport capacity of the renal tubules is not likely to be exceeded(29).

A five compartment model used in this research is diagrammed in

Figure 4. The first compartment represents the plasma pool that participates in OIH exchange with the proximal tubules of the kidneys. There are two pathways from compartment one. The first pathway to compartment five represents the I-131 OIH which is not cleared by the kidneys due mainly to binding of OIH to red blood cells. The differential equations describing the exchange of OIH into and out of the plasma and red blood cells are:

$$d[Q]_1/dt = k_5 * Q_5 - (k_1 + k_6) * Q_1 \quad (4)$$

$$d[Q]_5/dt = k_6 * Q_1 - k_5 * Q_5 \quad (5)$$

where, $[Q]_1$ and $[Q]_5$ represent the counts from I-131 OIH detected in the plasma and extra-plasma pool respectively. The rate constant k_5 (min^{-1}) represents the proportion of I-131 OIH per minute flowing from compartment five to compartment one, while k_6 (min^{-1}) represents the proportion of I-131 OIH per minute flowing from compartment one to compartment five.

The second pathway from compartment one represents the plasma clearance of OIH into the right and left proximal tubular cells. By multiplying k_1 (min^{-1}) by the plasma volume, the volume of plasma cleared by both kidneys in one minute is obtained, commonly called the effective renal plasma flow. The fraction k_2 , represents the proportion of I-131 OIH going to the left kidney (compartment two) while $(1-k_2)$ represents the proportion going to the right kidney (compartment three). The differential equations describing OIH clearance by the kidneys are:

$$d[Q]_2/dt = k_1 * k_2 * Q_1 - k_4 * Q_2 \quad (6)$$

$$d[Q]_3/dt = k_1 * (1-k_2) * Q_1 - k_3 * Q_3 \quad (7)$$

where $[Q]_2$ and $[Q]_3$ represent the counts from I-131 OIH detected in the

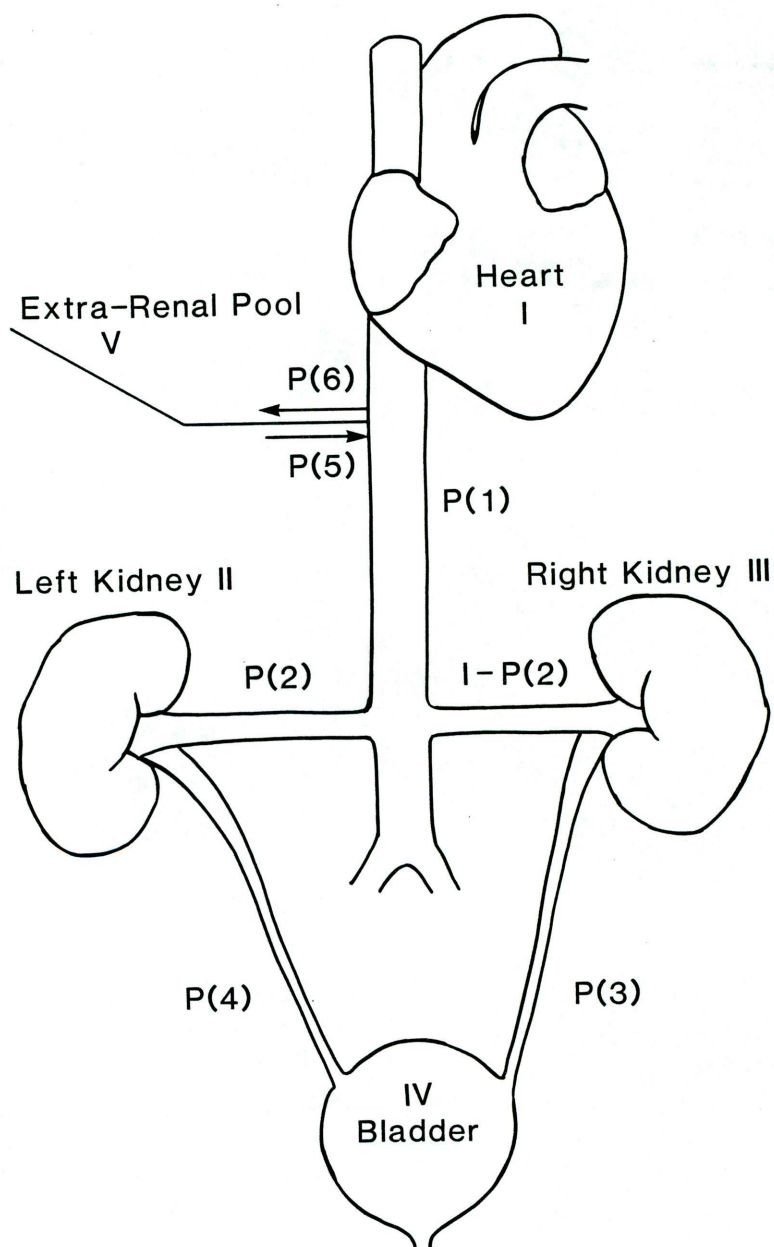


Figure 4. Diagram representing a five compartment model of the mammalian renal system. The rate constants $P(1)$, $P(2)$, $P(3)$, $P(4)$, $P(5)$ and $P(6)$ shown on the diagram correspond to k_1 , k_2 , k_3 , k_4 , k_5 and k_6 , respectively, in the text.

left and right kidneys respectively.

The fourth compartment represents the bladder. Inputs from the right and left kidneys are represented by k_3 (min^{-1}) and k_4 (min^{-1}) respectively. The differential equation describing the flow of urine to bladder is:

$$d[Q]_4/dt = k_4 * Q_2 + k_3 * Q_3 \quad (8).$$

The rate constant k_3 (min^{-1}) represents the proportion of OIH in urine flowing from compartment three to compartment four. The rate constant k_4 (min^{-1}) represents the proportion of OIH in urine flowing from compartment two to compartment four.

Solution of Equations

Equations 4-8 were solved using a program package for simulation and parameter estimation in kinetic systems developed by D'Argenio and Schumitzky(18). This package was written to handle linear and non-linear, multiple input, multiple output compartment models and allows for both rate inputs and bolus type inputs such as is used in the model of this research. With this package, any model which can be represented by ordinary differential equations and whose inputs are piecewise constant or can be simulated by state jump conditions may be used(18).

Programs developed by Shampine and Gordon(50) using the variable order, variable step integration routine of the Adam's methods are used for solving the differential equations. The adaptive simplex method of Nelder and Mead(37) is applied as the parameter estimation procedure to solve for unknown parameters k_1 , k_2 , k_3 and k_4 . The Nelder-Mead procedure minimizes a weighted least squares criterion and has been used on noisy data, such as the data encountered in this project, with

excellent results(18,39).

The package of programs were received on magnetic tape courtesy of Dr. Alan Schumitsky at the University of Southern California in Los Angeles. All programs were written in Fortran utilizing double precision arithmetic and were running on a DEC KL-10 computer at the University of Southern California. The programs had to be converted to run on the Data General Eclipse S/200 system in the Scientific Computation Facility at Loma Linda University Medical Center.

In order to limit the memory requirement for the parameter estimation program while maintaining double precision arithmetic, the limits for the program variables had to be decreased. The programs now allow 5 states, 5 rate inputs, 5 bolus inputs, 5 dose events, 125 total observations for all outputs, 5 outputs and 15 model parameters. Many of the programs and subroutines had to be divided into smaller sections and chained together passing necessary values in data files. Following successful loading of the converted programs into the Data General Eclipse System, the accuracy of the conversion was verified by comparing the results of sample runs provided in D'Argenio and Schumitsky's publication(18) to the output from the converted programs.

Inputs to the Model

When working with compartmental analysis, it is common to observe the concentration of a substance in one or more compartments as a function of time and then try to deduce the parameters of the system from the observed behavior of this substance. This compartmental model was written to be used in this way with clinical data.

In a nuclear medicine department, a patient is given a bolus

injection of I-131 OIH while simultaneously detecting the photons emitted by the I-131 as it passes through different organ systems. NaI (Tl) scintillation detectors are used to detect these photons. In this research, two scintillation probes manufactured by Technical Associates were used, one positioned anteriorly over the heart and the other positioned anteriorly over the bladder. Each probe was connected to an ORTEC single channel analyzer which analyzes each signal for the I-131 energy and records these counts for specified units of time. The output of the heart probe becomes the model input, $[Q]_1$, per unit time. The output of the bladder probe becomes the model input, $[Q]_4$, per unit time. Both inputs $[Q]_1$ and $[Q]_4$, were corrected for background counts recorded for each probe prior to injection. In addition, a NaI(Tl) scintillation gamma camera with a high energy collimator, was used to detect I-131 OIH as it passes through the kidneys.

The Searle, standard field of view, gamma camera was connected through a single channel analyzer and an analog-to-digital converter to a NOVA III mini-computer. The computer recorded not only the counts from each kidney but also the X-Y position of where each count came from in the field of view of the camera. This resulted in a two dimensional image of the kidneys for each time interval recorded. Typical acquisition time intervals for a study were for 12 seconds per frame acquired for 120 frames. With the computer, recorded kidney images can be summed over time and regions-of-interest for each kidney can be flagged so that only counts from the left kidney region were used to make a time/activity curve and, similarly, only counts from the right kidney region were used to make another time/activity curve. A background

region of interest was also flagged in an area free of other organs such as liver or ureters. A time/activity curve for the background region was plotted and after normalization for the different size areas for each region, the background curve was subtracted from each kidney curve. The corrected left kidney time/activity curve was the input $[Q]_2$. The corrected right kidney time/activity curve was the input $[Q]_3$. Diagrams of regions and examples of time/activity curves can be found in chapter three.

An input representing counts from a bolus of activity of I-131 OIH was introduced into compartment one at time zero. The bolus count was the value of the y-intercept found by extrapolating the time/activity curve recorded from the heart probe back to intercept the y-axis at time zero.

It should also be noted that inputs $[Q]_1$, $[Q]_2$, $[Q]_3$ and $[Q]_4$ start at one minute. This time lapse allows for deposition of I-131 OIH into erythrocytes at the same time plasma mixing was taking place(19) and also insured that the background activities were proportional to the blood concentration of I-131 OIH(29).

Parameters k_1 through k_4 , discussed earlier, were the unknowns solved for by the parameter estimation routine. The rate coefficients, k_6 and k_5 , representing flow into and out of compartment five respectively have been found by repeated analyses to be similar for all situations tested. For this reason, k_6 was held constant at 1.0/min and k_5 was held constant at 2.5/min. These values were in agreement with similar measurements by others(19,32). Since the rate coefficients describing flow into and out of compartment five were held constant and

since it would be very difficult to sample the red cell compartment, the input $[Q]_5$ was initially set to 1.0 for all sample times.

To test this compartmental model, animal experiments were performed in which normal and surgically induced abnormal clinical situations were tested. The quantitative clearance parameters calculated with the model were compared to clearance values obtained in the more conventional PAH and inulin clearance studies performed simultaneously. The next chapter describes these experiments and reports the results of these analyses.

CHAPTER 3

ANIMAL EXPERIMENTS: TESTING THE MATHEMATICAL MODEL

Design of Experiments

Initially, it was proposed to use female goats as the animal model. Goats were chosen because they are tolerant of indwelling catheters for prolonged periods of time (66). The experiments were initially set up so that by sterile surgery, catheters would be placed in an artery, the renal veins and both ureters of a goat with normal kidneys. Clearance studies and I-131 OIH renography would then be performed. After sufficient recovery, the animal would again undergo surgery to induce an abnormal kidney condition. The clearance studies and the I-131 OIH renography would then be repeated. In this way, the abnormal values could be compared to normal values for the same animal. However, the problems of keeping the catheters in the correct position and free from clots, as well as, keeping the animal free from infection were insurmountable and it was decided that an acute model should be used to replace the chronic model.

Dogs were chosen as the animal model for the acute studies, since dogs have been successfully used for renal function studies by many investigators in the past as referenced in Chapter one. To test the compartment model, simultaneous standard PAH and inulin clearance studies for each kidney were run immediately prior to I-131 OIH renography so that clearance parameters calculated by the model could be compared to the PAH and inulin clearances. Dogs with normally functioning kidneys

were first to undergo the procedure. Afterwards, several surgically induced abnormal conditions were tested, including, total ureteral obstruction, renal vein occlusion, a segmental infarct by ligating a branch of the renal artery, renal artery stenosis and acute renal failure induced by injecting a nephrotoxin. When possible the abnormal conditions were induced in only one kidney, leaving the contralateral kidney unaffected for normal comparison.

Experimental Protocol

Surgical Protocol

Both male and female mongrel dogs ranging in weight between 24 and 40 kg, were used for these studies. The dogs were anesthetized using sodium pentobarbital (30mg/kg body weight) administered intravenously. A catheter was placed in the jugular vein for administration of drugs and replacement of fluids. The abdomen was surgically opened, the bladder was dissected and catheters placed into both ureters and tied in place. Following a cut-down procedure, under fluoroscopy, catheters were placed in the aorta via the left or right femoral artery and in both renal veins via the left and right femoral veins. In the animals with both kidneys functioning normally, only one renal vein was catheterized. It was assumed that the concentration of PAH and inulin would be equal in the left and right renal veins of normal kidneys. Saline was then infused to achieve a urine flow rate of 1-3 cc/minute.

PAH and Inulin Clearance Studies

The PAH and inulin clearance studies were performed first, to

prevent radioactive contamination of laboratory equipment. Blood samples from the arterial and renal veins were drawn and twenty minute urine collections were made prior to injecting PAH or inulin to be used as baseline values for PAH and inulin concentrations. A primary loading dose of PAH (8 mg/kg) and inulin (50 mg/kg) was then administered followed by a sustained infusion of 0.27 mg/kg/min of PAH and 1.1 mg/kg/min of inulin (54). After initiation of the infusion doses and a thirty minute period for equilibrium, three successive twenty minute urine collections were obtained. Arterial and renal vein blood samples were withdrawn at the mid-point of each urine collection period. Red cells and plasma were separated by centrifugation.

Concentrations of PAH and inulin in plasma and urine samples were analyzed using standard colorimetric methods (1). The effective renal plasma flow for each kidney was calculated from PAH concentrations using the following formula from Pitts (41):

$$\text{ERPF}_{\text{total}} \text{ (ml/min)} = \frac{(U-VP) * V}{(AP - VP)} \quad (9)$$

where,

U = urine concentration of PAH (mg/dl)

VP = renal vein plasma conc. of PAH (mg/dl)

AP = arterial plasma conc. of PAH (mg/dl)

V = volume of urine collected per minute (ml/min)

Glomerular filtration rate for each kidney was calculated using inulin concentrations using the following formula from Pitts (41):

$$\text{GFR}_{\text{total}} = \frac{U * V}{VP} \quad (10)$$

where,

U = urine concentration of inulin (mg/dl)

VP = renal vein plasma conc. of inulin (mg/dl)

V = volume of urine collected per minute (ml/min)

Radionuclide Studies

Prior to injecting I-131 OIH, the animal's plasma volume was measured by the I-125 albumin dilution method (21). The hematocrit was also evaluated. The animal was placed in a supine position over the gamma camera. One NaI (Tl) scintillation probe was positioned over the heart and another probe was positioned over the "bladder." Since the bladder had been dissected during surgery to insert ureteral catheters, a plastic cup into which both catheters drained was used to simulate the bladder. A 500 microcurie Tc-99m glucoheptonate dose was then injected to localize and position the kidneys to ensure they were in the field of view of the gamma camera.

The radionuclide renal clearance study was then performed by injecting a bolus of I-131 OIH (4.4 μ Ci/kg) while simultaneously collecting counts from both probes and the gamma camera as the radiopharmaceutical passed through each compartment. The data was collected in twelve second intervals for twenty-five minutes. The counts per 12 seconds from the heart and bladder probes were printed out separately to be used as time/activity curve inputs for compartments one and four, respectively.

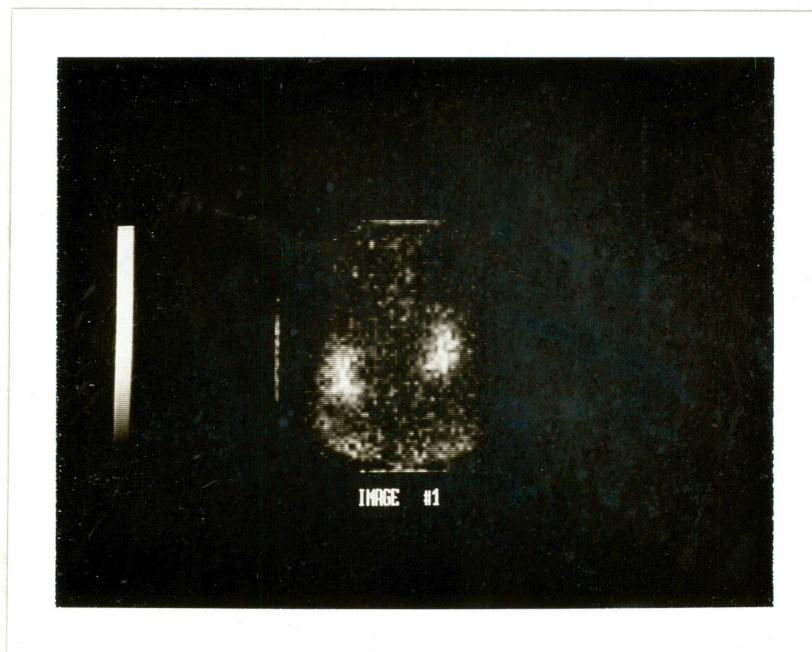
As stated previously, images of the kidneys from the gamma camera were recorded on a digital computer. These images were summed and regions of interest flagged for each kidney, as well as, a background

region of interest, as depicted in figure 5. These kidney regions were then used to plot time/activity curves corrected for a normalized background count. Figure 6 graphically illustrates time/activity curves from both kidneys, the heart and bladder from a dog with normally functioning kidneys and from a dog with total left ureteral obstruction.

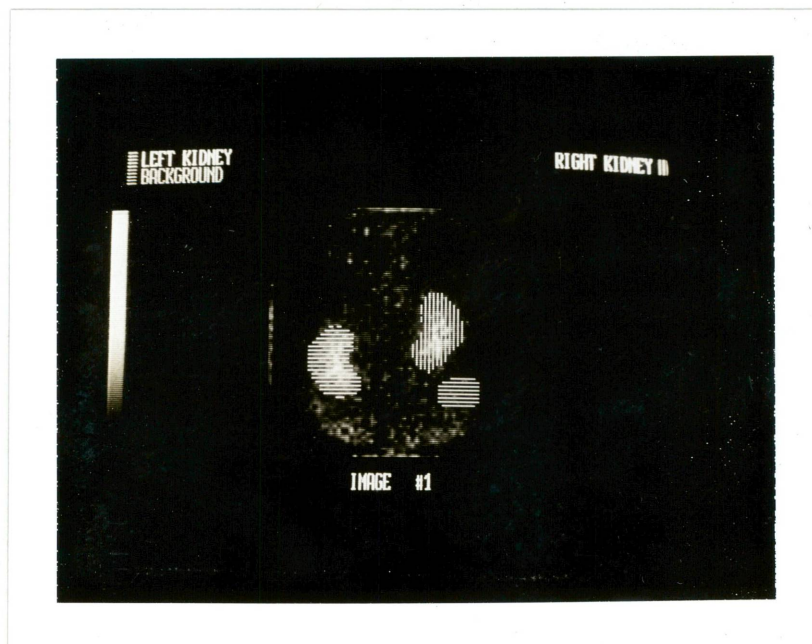
In addition to obtaining time/activity curves from kidney regions of interest, additional processing of the computer images of the kidneys was done. Each of the 120 images of the kidneys was filtered using digital temporal and low-pass spatial filters available on software provided on the Medical Data Systems NOVA III minicomputer used in the Nuclear medicine department. Through experimentation, using filters of various neighborhoods and cut-off frequencies, it was found that for both the temporal and low-pass spatial filter, using a neighborhood of 7 and a cut-off frequency of .15 cycles/sample eliminated the background counts and gave the overall best results. After filtering, a Fourier analysis was done on the images. This phase analysis was also available on existing software from Medical Data Systems NOVA III minicomputer.

The filtering and Fourier analysis on the series of kidney images showed the dynamic pattern of blood flow through the kidneys. The phase diagrams were color coded so that counts corresponding to blood activity were represented by the same color when found to be at the same phase angle. As the phase angle changes, so that the color scale changes, a representation of the pattern of blood flow through the kidney was seen. This colored pattern can be shown in a dynamic display on the computer.

In these color coded phase diagrams, kidneys with normal function showed initial blood flow to the cortical regions represented by the red



Summed kidney images for a normal study.



Regions of interest drawn over the left and right kidneys with the background region drawn under the right kidney.

Figure 5

TIME/ACTIVITY CURVES OBTAINED FROM SCINTILLATION DETECTORS AS A BOLUS OF I-131 OIH WAS INJECTED INTO DOGS.

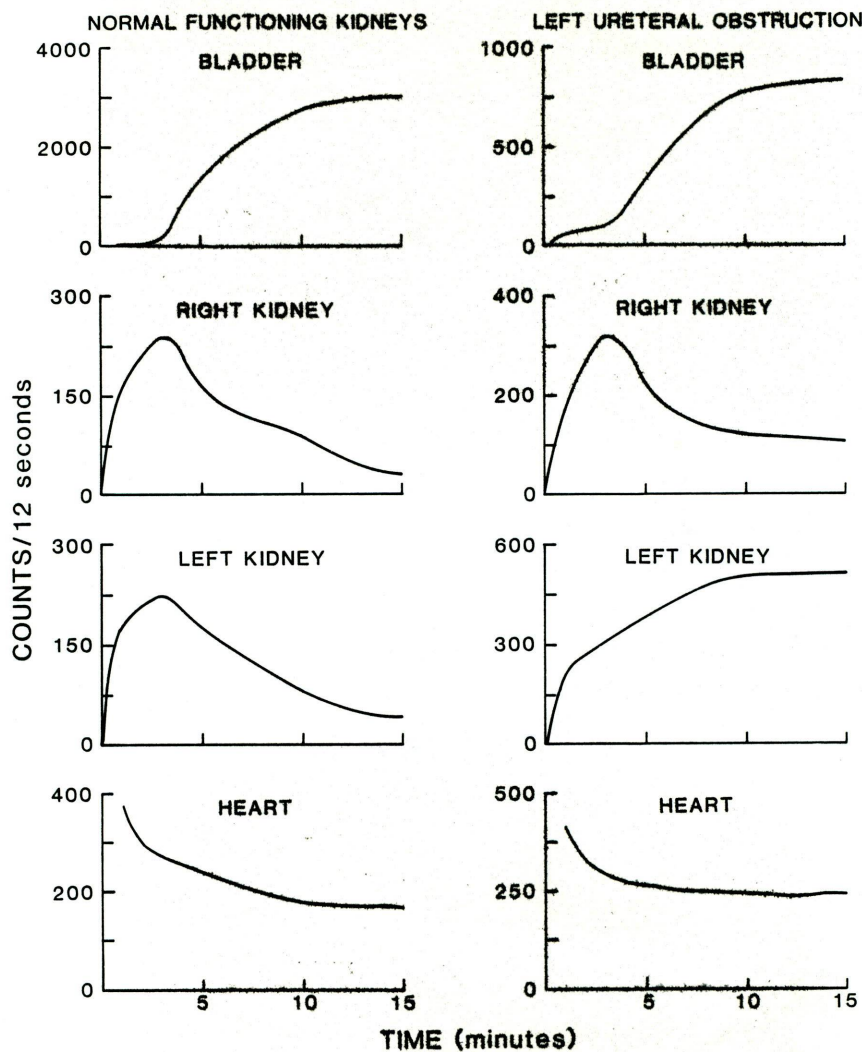
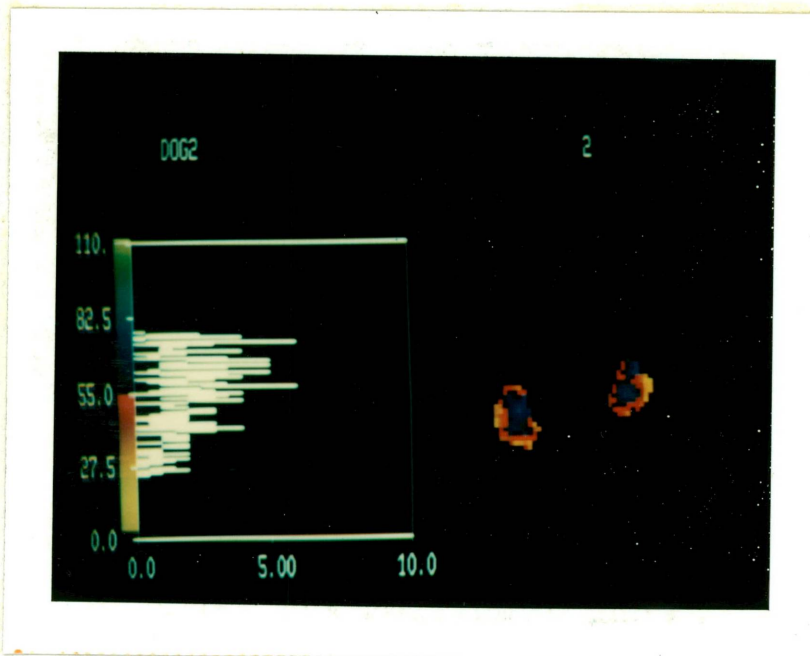
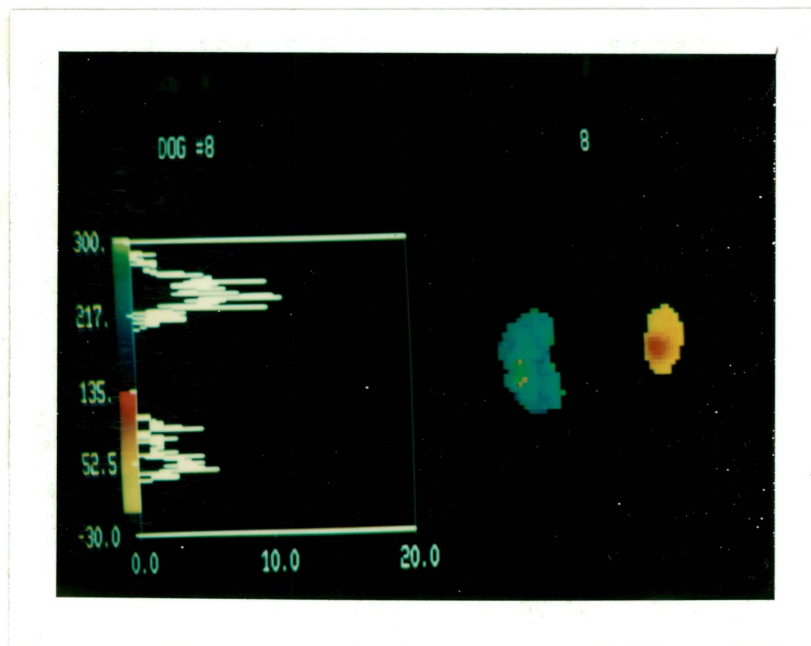


Figure 6

areas in figure 7, followed by flow to the medullary regions represented by the blue areas of the same figure. Figure 7 is the color coded phase diagram of a dog in which the left kidney had total ureteral obstruction. The normal right kidney showed the characteristic initial blood flow to



Phase images of normal kidneys. The red areas show initial blood flow to the cortex followed by blood flow to the medulla represented by the blue areas.



Phase images of kidneys in which the right kidney is normal and the left kidney has total ureteral obstruction. The right kidney shows normal initial blood flow to the cortex (yellow area) followed by blood flow to the medulla (red area). The obstructed left kidney (blue areas) shows delayed flow compared to the right kidney with no definite cortical and medullary areas.

Figure 7

the cortical region represented by the yellow area, followed by flow to the medullary region represented by the red area. The phase diagram showed delayed blood flow to the obstructed left kidney compared to the normal right kidney. The left kidney was represented as a blue color which was completely out of phase with the right kidney.

The time it takes for blood to flow from the cortex to the medullary region was calculated using the color coded regions of interest from the computer to plot time/activity curves. We have called the difference in peak times between the cortical curve and medullary curve, the cortex-to-medulla transit time. The transit time varied from 0.8 minutes to 3.2 minutes for the normal kidneys tested. The cortex-to-medulla transit time for the measurable abnormal kidneys tested varied from 0.6 minutes to greater than 20 minutes. Several of the abnormal kidneys had no blood flow through the kidney, therefore, cortex-to-medulla transit time could not be measured. Table 5 in a later section, lists the calculated cortex to medulla transit times and discusses the results for the studies reported.

Computer Printout of Model Parameter Estimation Routine

The time/activity curves obtained for both kidneys, the heart and bladder were then inputted to a file on the Data General Eclipse S/200 system to be used by the parameter estimation routines described in Chapter 2 to solve for k_1 , k_2 , k_3 and k_4 corresponding to P(1), P(2), P(3) and P(4), respectively, on the computer printout. Figure 8 was a sample printout of a computer run on study number two. After specifying the data input file name, the option to print information contained in this file was given.

COMPARTMENT MODEL IDENTIFICATION

```

ENTER THE INPUT FILE NAME:  DOG2
      MODEL INPUT INFORMATION
THE NUMBER OF RATE INPUTS:  0
THE NUMBER OF BOLUS INPUTS: 1
THE NUMBER OF DOSE EVENTS:  1
      DOSAGE REGIMEN INFORMATION
EVENT      TIME      RATE AND/OR AMOUNT FOR ALL INPUTS
           UNITS,      B(1)
1          0.0          4424.00

      MODEL OUTPUT INFORMATION
THE NUMBER OF MODEL OUTPUTS:  5
THE NUMBER OF OBSERVATION TIMES: 96
DO YOU WANT OBSERVATIONS PRINTED? N

      SUPPLY DATA WEIGHTING INFORMATION
      OUTPUT WEIGHTS
SUPPLY THE WEIGHTS FOR EACH OUPUT, Y(1)---Y(5):
1.0,1.0,1.0,1.0,1.0

      OBSERVATION WEIGHTS
THE FOLLOWING OBSERVATION WEIGHTING SCHEMES ARE AVAILABLE:
1. GENERAL WEIGHTING.
2. INVERSE VARIANCE OF THE ASSAY WEIGHTING. (LINEAR)
3. INVERSE VARIANCE OF THE ASSAY WEIGHTING. (NONLINEAR)

FOR Y(1):
  ENTER THE NUMBER OF THE DESIRED WEIGHTING PROCEDURE:  1
  ENTER THE NUMBER OF NON-UNITY WEIGHT OBSERVATIONS:    0

FOR Y(2):
  ENTER THE NUMBER OF THE DESIRED WEIGHTING PROCEDURE:  1
  ENTER THE NUMBER OF NON-UNITY WEIGHT OBSERVATIONS:    0

FOR Y(3):
  ENTER THE NUMBER OF THE DESIRED WEIGHTING PROCEDURE:  1
  ENTER THE NUMBER OF NON-UNITY WEIGHT OBSERVATIONS:    0

FOR Y(4):
  ENTER THE NUMBER OF THE DESIRED WEIGHTING PROCEDURE:  1
  ENTER THE NUMBER OF NON-UNITY WEIGHT OBSERVATIONS:    0

FOR Y(5):
  ENTER THE NUMBER OF THE DESIRED WEIGHTING PROCEDURE:  1
  ENTER THE NUMBER OF NON-UNITY WEIGHT OBSERVATIONS:    96
  ARE ALL NON-UNITY WEIGHTS EQUAL TO ZERO?              Y

```

Figure 8. Computer printout of the Parameter Estimation Routine.

SUPPLY MODEL EQUATION INFORMATION

ENTER THE NUMBER OF DIFFERENTIAL EQUATIONS: 5
 ENTER THE COMPARTMENT NUMBER FOR EACH BOLUS INPUT: 1
 ENTER THE NUMBER OF MODEL PARAMETERS: 6

ENTER PARAMETER ESTIMATES & SPECIFY THOSE TO BE ADAPTED:
 ESTIMATE ESTIMATE

P(1)	.3	IC(1)	0
ADAPT? Y		ADAPT? N	
P(2)	.5	IC(2)	0
ADAPT? Y		ADAPT? N	
P(3)	.5	IC(3)	0
ADAPT? Y		ADAPT? N	
P(4)	.5	IC(4)	0
ADAPT? Y		ADAPT? N	
P(5)	1.0	IC(5)	0
ADAPT? N		ADAPT? N	
P(6)	2.5		
ADAPT? N			

ENTER MAXIMUM NUMBER OF ITERATION: 99
 DO YOU WANT ITERATIONS PRINTED? N

RESULTS

A. ITERATIONS

ITERATION 0
 NUMBER OF FUNCTION CALLS = 1
 ADAPTED PARAMETERS
 P(1) = .30000
 P(2) = .50000
 P(3) = .50000
 P(4) = .50000

B. ITERATION SUMMARY

CONVERGENCE HAS BEEN ACHIEVED

NUMBER OF ITERATIONS = 19
 NUMBER OF FUNCTION CALLS = 95
 ADAPTED PARAMETERS
 P(1) = .35660
 P(2) = .51295
 P(3) = .55011
 P(4) = .55453

Figure 8 - cont.

Observation weighting scheme 1 was then selected. The general weighting scheme allows the user to enter directly the observation numbers and the associated weights for any or all of the observations. Since there was more than one compartment sampled, it was necessary to assign a weight to each output since each may represent different quantities or may be measured on different scales. A weight of unity was given to all observations unless specified otherwise. Since the red cell compartment cannot be sampled, observations for compartment five were inputted at a value of 1.0. The weights for these observations were then set to zero so as not to affect the other parameter estimates. The general weighting scheme was chosen as recommended for observations which have a constant variance (18).

The number of differential equations, the compartment number for the bolus report, estimates for each parameter and the option to adapt each parameter was then inputted.

A summary of the iteration after convergence was achieved, was then printed out. Values for the four adapted parameters were given.

Results and Discussion of Parameter Estimates

Table 1 is a listing of the values for each of the four parameters calculated for all of the studies reported. It should be noted that for the two parameters, P(3) and P(4), it was found that when running the parameter estimation routine after fixing P(3) and P(4) at values ranging from .05 to 1×10^{-6} for various studies, that values less than .01, for either parameter had no affect on values estimated for the remaining parameters. Therefore, estimated values less than .01 for parameters

TABLE 1
ESTIMATED MODEL PARAMETERS

STUDY NO.	P(1) (min ⁻¹)	P(2) FRACTION TO LEFT KIDNEY	1 - P(2) FRACTION TO RIGHT KIDNEY	P(3) (min ⁻¹)	P(4) (min ⁻¹)	COMMENTS
2	.35660	.51295	.48705	.55011	.55453	Normal
3	.32703	.51136	.48864	.44651	.44684	Normal
5	.30561	.57360	.42640	.37554	.42963	Normal
6	.35839	.43540	.56460	.42299	.48952	Normal
7	.33723	.56516	.43484	.44381	.44890	Normal
8	.15019	.37128	.62872	.26455	.01	Left ureteral obstruction
9	.22860	.09405	.90595	.71128	.01	Left renal vein occlusion.
10	.16951	.11974	.88026	.53495	.01	Left renal vein occlusion. Right renal artery branch occlusion
12	.18296	.40361	.59639	.25049	.21824	Left renal artery stenosis
13	.27167	.25543	.74457	.50755	.20754	Left renal artery branch occlusion
14	.05192	0	1	.11305	0	Nephrotoxin admin. bilat.
15	.34201	.31627	.68373	.29137	.26623	Left renal artery branch occlusion
16	.18864	.13768	.86232	.44655	.01	Nephrotoxin admin., left unilaterally

P(3) and P(4) were reported as .01. This change affected studies 8, 9, 10, and 16 for parameter P(4).

The mean value and standard deviation at the 95% confidence level for P(1) for the normal studies 2-7 was reported to be $.337 \pm .040 \text{ min}^{-1}$. The remaining values for P(1) for the abnormal studies decreased corresponding to a decreased total effective renal plasma flow.

The mean value and standard deviation at the 95% confidence level for P(2) and 1-P(2) for the normal studies 2-7 was reported to be $.500 \pm .106$. These parameters, representing the fraction of total effective renal plasma flow to the left and right kidney, respectively, were expected to be .5 since half the blood flow was expected to go to each kidney for normal function. The values for P(2) for the abnormal kidneys were decreased significantly, as expected with corresponding increases in the fraction of total to the right kidney. Parameters P(1), P(2) and 1-P(2) will be discussed in more detail in the next section.

The mean value and standard deviation at the 95% confidence level for P(3) and P(4) for the normal studies was reported to be $.461 \pm .10 \text{ min}^{-1}$. These parameters which were proportional to the urine flow from the right and left kidneys respectively, decreased for the abnormal studies as expected. P(3) and P(4) will also be discussed in more detail in the next two sections.

Results and Discussion of Predicted Effective Renal Plasma Flow Estimates

Table 2 compares the PAH clearances to the ERPF's predicted by the model and Table 3 gives the results of the inulin clearance tests. The normal value for PAH clearance for female dogs was reported to be $13.5 \pm$

TABLE 2
PAH CLEARANCES COMPARED TO PREDICTED ERPF'S

STUDY NO.	PAH CLEARANCES (ml/min/kg)	PREDICTED ERPF (ml/min/kg)	LEFT PAH CLEARANCE (ml/min/kg)	LEFT PREDICTED ERPF (ml/min/kg)	RIGHT PAH CLEARANCE (ml/min/kg)	RIGHT PREDICTED ERPF (ml/min/kg)	COMMENTS
2	18.5	19.8	9.5	10.1	9.1	9.7	Normal
3	18.4	16.9	12.5	8.6	6.0	8.3	Normal
5	10.5	14.0	4.7	8.0	5.8	6.0	Normal
6	20.4	17.5	10.8	7.6	9.6	9.9	Normal
7	13.5	18.2	7.2	10.3	6.3	7.9	Normal
8	5.6	6.3	NU	2.3	5.6	3.9	Left ureteral obstruction
9	6.2	9.2	NU	.87	6.2	8.4	Left renal vein occlusion
10	NA	8.3	NU	.99	NA	7.3	Left renal vein occlusion. Right renal artery branch occlusion
12	11.1	8.9	2.0	3.6	9.1	5.3	Left renal artery stenosis
13	5.5	12.8	.85	3.3	4.6	9.5	Left renal artery branch occlusion
14	.03	1.8	NU	0	.03	1.8	Nephrotoxin admin. bilat.
15	12.0	12.8	4.6	4.1	7.4	8.7	Left renal artery branch occlusion
16	7.1	6.8	NU	.94	7.1	5.9	Nephrotoxin admin., left unilaterally

NA - Values not available due to clotted catheter

NU - Values not available due to no urine formation

TABLE 3
TABLE OF INULIN CLEARANCES (GFR)

STUDY NO.	INULIN CLEARANCE (ml/min/kg)	LEFT INULIN CLEARANCE (ml/min/kg)	RIGHT INULIN CLEARANCE (ml/min/kg)	FILTRATION FRACTION $\left[\frac{C_{IN}}{C_{PAH}}\right]$	COMMENTS
2	4.8	2.4	2.4	26%	Normal
3	7.2	4.1	3.1	39%	Normal
5	3.4	1.5	1.9	32%	Normal
6	5.6	2.9	2.7	27%	Normal
7	6.1	3.5	2.6	45%	Normal
8	.76	NA	.76	14%	Total left ureteral obstruction
9	3.9	NA	3.9	63%	Total left renal vein ligation
10	NA	NA	NA	NA	Right renal artery branch ligation-left renal vein ligation
12	2.9	.4	2.5	26%	Left renal artery stenosis
13	1.9	.7	1.2	34%	Left renal artery branch ligation
14	.0001	NA	.0001	.3%	Nephrotoxin admin. bilat.
15	3.0	1.9	1.1	25%	Left renal artery branch ligation
16	.76	NA	.76	11%	Nephrotoxin admin., left unilaterally

In studies 8, 9, 10, and 14, no urine was available for analysis from the left kidney and in study 10, no blood could be drawn from the catheter placed in the right renal vein.

3.26 ml/min/kg from Smith (52). The normal value for inulin clearance for female dogs was reported to be 4.3 ± 1.01 ml/min/kg from Smith (52). It was assumed that similar to humans, the PAH and inulin clearances for male dogs would be higher. The mean value and standard deviation at the 95% confidence level for the PAH clearance in the three normal male dogs evaluated in this study was 16.5 ± 4.3 ml/min/kg and 15.9 ± 2.5 ml/min/kg in two normal female dogs studied. The range of PAH clearances in normal female dogs found in this study was within the reported normal range found in the literature. Two dogs evaluated for this study as normals were not included in the data since the laboratory analyses for PAH were in error and the PAH clearances calculated, far exceeded the normal range.

Comparing the predicted ERPF's to the PAH clearances, for normal and abnormal studies 2-16, we found the correlation coefficient, r , to be 0.88. The study with the largest difference between the PAH clearance and the predicted ERPF was study number 13. Excluding number 13, the correlation coefficient for studies 2-16 was 0.92. We were unable to determine the reason for such a large error for study number 13. Therefore, it was repeated.

For studies 8, 9, 10, 14 and 16, the surgically induced abnormality to the left kidneys caused these kidneys to become anuric. Since the analytical analyses for PAH and inulin clearances depend on urine concentrations, no PAH and inulin clearances could be calculated for the above mentioned studies.

In study number 8, total left ureteral obstruction was produced by ligating the ureter from the left kidney. The right kidney was normal. The basic mechanism for altered renal function in urinary tract

obstruction was a decrease in urine flow and an increase in pressure in the renal tubule, resulting in decreased ERPF and glomerular filtration (68). As expected, the PAH clearance was markedly decreased. The predicted total ERPF was also markedly decreased, following the PAH clearance. The left kidney PAH clearance could not be calculated due to postrenal anuria. The model predicted an abnormally low left kidney ERPF as expected and normal right kidney ERPF. Also as expected, the model predicted a very small value for $P(4)$, which represents urine flow from the left kidney. In this study, the blood flow to the left kidney was somewhat reduced while the urine flow from the left kidney was drastically reduced.

In study number 9, total left renal vein occlusion was surgically induced by ligating the left renal vein. The right kidney was normal. Renal vein occlusion has been known to cause a decline in renal function by decreasing both the ERPF and GFR with resulting oliguria and anuria for the affected kidney (20). The degree of decline in renal function was largely dependent on the degree of the occlusion. As expected in this study, the PAH clearance was reduced, followed by a reduced predicted ERPF. The left kidney PAH clearance could not be calculated since no urine was produced. The predicted left kidney ERPF was drastically reduced (10% of normal) while the predicted right kidney ERPF was normal. In addition, $P(4)$ was also a very small value, predicting very little urine flow from the left kidney as would be expected with severely reduced kidney function. The GFR of the right kidney was elevated which may be a response to the left kidney problems. In this study, both the

blood flow to the left kidney and the urine flow from the left kidney were both drastically reduced.

In study number 10, total left renal vein occlusion was surgically induced by ligating the left renal vein, similar to study number 9. Again as expected, the predicted total ERPF was reduced, however no PAH or inulin clearance could be calculated for comparison since the catheter placed in the right renal vein became clotted and no urine was produced from the left kidney. The predicted left kidney ERPF was again drastically reduced (15% of normal) with a very small value of $P(4)$ representing little urine flow from the left kidney. These results compare favorably to the results found in study number 9, showing consistency in the model predictions.

In addition, for study number 10, a segmental infarct to the right kidney was induced by ligating a branch of the right renal artery. An infarct results in a loss of renal function shown by a decrease in the ERPF accompanied by a decrease in urine output (20). The degree of decline in renal function depends on the degree of the infarct. Since we do not have a PAH clearance for the right kidney, we have no comparison for the predicted right kidney ERPF. A comparison with other kidneys in which segmental infarcts were induced will be made in a later section discussing the blood to urine flow index.

In study number 12, renal artery stenosis was induced in the left kidney by partial clamping of the left main renal artery. The clamp was tightened on the left artery until the urine output from the left kidney was reduced to one third of the urine output from the right kidney. Using a flowmeter, the stenosis was estimated to be 65-75%. The right

kidney was normal in this study. Mild to moderate unilateral renal artery stenosis may cause little or no change in total renal function as determined by inulin and PAH clearance tests however, diminution of urinary volume may occur and become more marked as the stenosis becomes more severe (20). As the stenosis becomes more severe, the decrease of ipsilateral blood flow was countered by an increase in blood flow to the contralateral kidney (20). Using conventional radio-renograms, unless the stenosis was quite severe, 80% or more, no changes are seen in the renogram curves (5). The total PAH clearance for study number 12, was moderately reduced with the left PAH clearance being reduced while the right kidney PAH clearance was elevated slightly. Also, the left kidney inulin clearance (GFR) was reduced while the right kidney inulin clearance (GFR) was elevated. As explained above, this may be expected for a severe stenosis. The predicted total ERPF was reduced following the PAH clearance. However, the predicted left kidney ERPF was not reduced as much as the corresponding left PAH clearance and the predicted right kidney ERPF was not elevated as was the corresponding right PAH clearance. The parameter, P(4), representing left urine flow, was less than P(3), representing right urine flow, which may be expected for stenosis. One explanation for these differences in predicted ERPF and PAH clearances was that the radionuclide evaluation may not be as sensitive as the chemical evaluations. As stated earlier, unless a severe stenosis of at least 80% was present, little or no changes are seen in the radionuclide curves. Although the model predicted some decreased left kidney function, the model may be limited in evaluating less severe degrees of renal artery stenosis.

In study number 13, a segmental infarct to the left kidney was induced by ligating a branch of the renal artery, similar to the right kidney of study number 10. The right kidney for study number 13 was normal. The PAH clearance was drastically reduced (less than half of normal) whereas, the predicted total ERPF was only slightly reduced from normal. A 55% difference in these values was noted, however, no reason for this large difference could be attributed except for a possible error in the laboratory PAH analysis or overestimation by the model. The PAH clearance and predicted ERPF for the left kidney both showed reduced function compared to the right kidney. In addition, the inulin clearance for the left kidney was reduced as expected. The parameter, P(4), was also reduced representing decreased urine flow from the left kidney. In this study, the PAH clearance and predicted ERPF, both showed decreased left kidney function as expected, however, the precision of the quantitative comparisons was not good. The study was repeated for this reason in study number 15.

In study number 15, again a segmental infarct to the left kidney was induced. The total PAH clearance was slightly reduced as expected. The predicted total ERPF was also slightly reduced corresponding to the decrease in blood flow to the left kidney. For this study, the values for PAH clearance and ERPF agreed quite well. The difference in these values was small (6%) providing a higher precision than for study number 13 and still followed the pathology as well. The left kidney PAH clearance and predicted ERPF agreed and both showed decreased blood flow to the left kidney as expected. The right kidney values were within the normal range. The left kidney GFR was not reduced as expected. The

parameter, $P(4)$, was also slightly reduced corresponding to a reduced urine flow from the left kidney as expected, due to decreased function.

In study number 14, acute renal failure was induced by injecting a nephrotoxin. The nephrotoxin used for this study was uranyl nitrate. Acute renal failure was induced as recommended by Flamenbaum, by injecting uranyl nitrate, 10 mg/kg body weight, in a saline solution (22). Since unilateral acute renal failure was the objective, uranyl nitrate at the above dose level, was slowly injected into the left renal artery via a catheter placed under fluoroscopy. Immediately after the injection, fluoroscopy of the left kidney was performed. At this time, it was observed that the left kidney was in total acute renal failure. The possibility was noted that the nephrotoxin refluxed systemically and so affected the right kidney. Acute renal failure induced by uranyl nitrate is characterized by a decrease in both ERPF and GFR accompanied by oliguria and anuria (22). After studying the data from Flamenbaum (22), it was decided to perform the clearance studies and radio-renography twenty four hours after injection of the uranyl nitrate because all function parameters seemed to be reduced significantly by this time without large changes after twenty four hours. The left kidney was anuric at twenty four hours. As a result, PAH and inulin clearances could not be calculated for the left kidney. The right kidney had reduced urine output at twenty four hours. The PAH and inulin clearances for the right kidney were severely reduced as was the predicted ERPF, confirming that uranyl nitrate refluxed into the systemic circulation and affected the right kidney. The I-131 OIH renography recorded no activity in the left kidney. The input to the model for the left kidney

was therefore zero for all time intervals sampled. As a result, the predicted left kidney ERPF was zero. The parameter, $P(4)$, was zero representing no urine flow from the left kidney and the parameter, $P(3)$, was reduced corresponding to reduced urine flow from the right kidney. In this study, a severe acute renal failure was induced inadvertently affecting both kidneys. However, the model followed the pathology quite well. This study was repeated to test unilateral acute renal failure.

In study number 16, unilateral acute renal failure was induced by injecting a quarter of the previously injected dose (2.5 mg/kg) of uranyl nitrate into the left renal artery. Fluoroscopy of the left kidney showed decreased function immediately, however, refluxing into the systemic circulation was not observed. Twenty four hours later, the left kidney was not producing urine, therefore, PAH and inulin clearances could not be calculated. The right kidney had normal urine output. The I-131 OIH renography showed a small amount of activity in the left kidney. The predicted left kidney ERPF was severely reduced, while the predicted right kidney ERPF was within the normal range and agreed with the right kidney PAH clearance. The parameter, $P(4)$, was reported as a very small value indicating very little urine flow from the left kidney. $P(3)$ was within the normal range. The GFR calculated for the right kidney was reduced which may be explained if unobserved reflux of the nephrotoxin into the systemic circulation took place. In this study, in which unilateral acute renal failure was produced, the model followed the pathology predicting a decreased ERPF and decreased urine flow from the left kidney while the right kidney was predicted as normal.

Results and Discussion of the Blood-to-Urine Flow Index

The Blood-to-Urine Flow Index for each kidney was being defined in this research as the ratio of the model parameters which indicate blood flow into the kidney versus the urine flow out of the kidney. For the left kidney, the Blood-to-Urine Flow Index was equal to $P(2)/P(4)$. For the right kidney, the Blood-to-Urine Flow Index was equal to $1-P(2)/P(3)$. Table 4 is a listing of these ratios calculated for all reported studies. The mean value for the normal kidneys with the standard deviation at the 95% confidence level was 1.40 ± 1.02 . The normal kidneys included in this mean are the left kidneys for studies 2-7 and the right kidneys for studies 2-16 excluding studies 10 and 14. All normal kidneys had reported flow indexes within two standard deviations of the mean.

In study number 8 (left total ureteral obstruction), the blood flow into the left kidney decreased slightly while the urine flow was severely reduced. As a result, the left kidney flow index was very high, equal to 25 times above the mean.

In study number 9 (left total renal vein obstruction), both the blood flow into the left kidney and the urine flow out of the kidney were severely reduced with the urine flow more reduced than the blood flow. The resulting flow index was therefore higher than normal, seven times above the mean, but not as high as in study number 8.

In study number 10, the flow index for the left kidney (also with total renal vein occlusion) agreed with the left kidney flow index calculated in study number 9. The flow index was very successful in differentiating the two conditions induced in the left kidneys of studies

TABLE 4
LEFT AND RIGHT KIDNEY BLOOD-TO-URINE FLOW INDEXES

STUDY NO.	LEFT KIDNEY BLOOD-TO-URINE FLOW INDEX	RIGHT KIDNEY BLOOD-TO-URINE FLOW INDEX	COMMENTS
2	.92	.89	Normal
3	1.1	1.1	Normal
5	1.3	1.1	Normal
6	.89	1.3	Normal
7	1.3	.98	Normal
8	37.1	2.3	Left ureteral obstruction
9	9.4	1.3	Left renal vein occlusion
10	11.9	1.6	Left renal vein occlusion. Right renal artery branch occlusion
12	1.8	2.4	Left renal artery stenosis
13	1.2	1.5	Left renal artery branch occlusion
14	0	8.8	Nephrotoxin admin. bilat.
15	1.2	2.3	Left renal artery branch occlusion
16	13.8	1.9	Nephrotoxin admin., left unilaterally

8, 9 and 10. However, these studies represent extreme conditions, therefore, for less severe ureteral obstruction or renal vein occlusion, there will probably be a range of overlap in the values calculated for the flow index.

Also in study number 10, the right kidney (renal artery branch occlusion) showed both decreased ERPF and urine flow. In this condition, both parameters were decreased proportionately. As a result, the flow index was within the normal range as might be expected. This was also true for study numbers 13 and 15 in which left renal artery branch occlusion was induced.

In study number 12 (left renal artery stenosis), the left kidney showed a slightly decreased ERPF and decreased parameter for urine flow. With renal artery stenosis, as in study numbers 10 and 12, both parameters were decreased proportionately. Therefore, the flow index for the left kidney was within the normal range.

In study number 14, both kidneys were affected by the nephrotoxin. The left kidney was in total acute renal failure and the flow index was zero. In the right kidney, the urine flow was reduced more than the ERPF resulting in a higher than normal flow index, six times above the mean. In study number 16, the left kidney was affected more by the nephrotoxin. This kidney had an even lower urine flow with reduced ERPF resulting in a higher value for the flow index, ten times the normal mean.

Results and Discussion of the Cortex-to-Medulla Transit Time

The cortex-to-medulla transit time as discussed in a previous section was the peak to peak time difference of the cortex and medulla

time/activity curves. Table 5 lists the transit times for the reported studies. The mean value for the normal kidneys with the standard deviation at the 95% confidence level was $1.37 \pm .660$ minutes. The normal kidney values included in this mean were the left kidney transit times for studies 2-7 and the right kidney transit times for studies 2-16, excluding studies 10 and 14. All normal kidneys had reported transit times within two standard deviations of the mean, except the right kidney of study number 6. This variation may be due to the low counts observed for the cortex and medulla areas causing errors in the flagging process for obtaining the time/activity curves which were used for peak time determination.

In study number 8 (left ureteral obstruction), the transit time was delayed probably due to the increased pressure caused by the obstruction.

In studies 9 and 10 (left renal vein occlusion), the counts observed in these kidneys were very low so that the cortex and medulla could not be differentiated very well. The transit times are reported as infinity since the small amount of activity entering the kidney was not leaving.

In the right kidney of study number 10 and the left kidney of study number 13 in which segmental infarcts were induced, the transit times were within the normal range as might be expected since the I-131 OIH flowing through the unaffected segments of these kidneys was cleared normally. However, in study number 15, in which a segmental infarct had also been induced, the transit time was delayed, contradicting the above findings, but most likely due to low counting statistics.

In study number 12 (left renal artery stenosis), the transit time

TABLE 5
LEFT AND RIGHT KIDNEY CORTEX-TO-MEDULLA TRANSIT TIMES

STUDY NO.	LEFT KIDNEY CORTEX-TO-MEDULLA TRANSIT TIME (min)	RIGHT KIDNEY CORTEX-TO-MEDULLA TRANSIT TIME (min)	COMMENTS
2	1.2	.8	Normal
3	1.8	1.6	Normal
5	NA	NA	Normal
6	1.0	3.2	Normal
7	2.0	.8	Normal
8	> 20	.6	Left ureteral obstruction
9	∞	1.2	Left renal vein occlusion
10	∞	.8	Left renal vein occlusion. Right renal artery branch occlusion
12	2.0	1.8	Left renal artery stenosis
13	.6	.8	Left renal artery branch occlusion
14	∞	∞	Nephrotoxin admin. bilat.
15	5.2	1.2	Left renal artery branch occlusion
16	14.2	1.8	Nephrotoxin admin., left unilaterally

NA - Values not available due to loss of data.

∞ - Activity stays in the cortex.

was within the normal range of values. This might be expected for a moderate stenosis since little change in the renogram curve was observed.

In study number 14, in which both kidneys were affected by the nephrotoxin, no activity was observed in the left kidney, therefore, the transit time was reported as infinity. The activity seen in the right kidney of study number 14 stayed in the cortex, therefore, the transit time was reported as infinity for this kidney also.

In study number 16 (left kidney acute renal failure induced by a nephrotoxin), the transit time for the left kidney was delayed at ten times the normal mean.

CHAPTER 4

SUMMARY AND CONCLUSIONS

Summary

The model simulates OIH distribution and clearance in the renovascular system. This mathematical analysis describes the renal system as five compartments; the blood, left and right kidneys, bladder and the red blood cell compartment. The model takes into account the OIH trapped in the red blood cell compartment, even though this compartment cannot be directly monitored.

Data for the blood, kidney and bladder compartments are collected with scintillation detectors monitoring OIH tagged with I-131 as the radio-pharmaceutical passes through each compartment. The kidney data from the gamma camera are acquired onto a computer so that flagged regions of interest can be used to plot time/activity curves for each kidney. The heart, bladder and kidney data are then used as inputs to the model parameter estimation routine.

The compartments are described by a set of first-order ordinary differential equations. A method developed by Shampine and Gordon (50) using the Adam's methods is used to solve the equations. For parameter estimation, a method is used as developed by D'Argenio and Schumitsky (18) using an iterative predictor-corrector procedure. A Data General Eclipse S/200 system is used to carry out these calculations.

The estimated model parameters are used to calculate the quantitative values of total, left and right kidney effective renal

plasma flows. Two parameters are used as indications of urine flow. In addition, the Blood-to-Urine Flow Index is defined in this research using these parameters and is an indication of individual renal function. A cortex-to-medulla transit time is calculated using a Fourier analysis of the kidney images stored on the computer.

To verify the accuracy of the model, animal studies were done in which various kidney abnormalities were surgically induced. The abnormalities induced included, ureteral obstruction, renal vein occlusion, segmental infarcts, arterial stenosis and acute renal failure. The quantitative clearance parameters calculated by the model were then compared to clearance values received in PAH clearance studies performed simultaneously. Inulin clearances were also performed to substantiate the abnormalities.

Conclusions

Using this model, quantitative clinical estimates of renal function are possible. In addition, indications of urine flow, a Blood-to-Urine Flow Index, and cortex-to-medulla transit times are compared to help identify abnormal renal conditions which may be encountered in a clinical situation. Images obtained of the kidneys are helpful in identifying gross morphology.

The model predicts decreased effective renal plasma flow for all the abnormal conditions tested as expected. The predicted ERPF's decreased proportional to the degree of abnormality in the kidneys and correlated with an $r = .88$ with PAH clearances. The precision for these comparisons were not as good as might be expected. This limitation may be due to the accuracy of the laboratory analyses. The urine flows for

all the abnormal conditions were also decreased proportional to the degree of abnormality as expected.

Of particular interest is the Blood-to-Urine Flow Index. The flow index was successful in differentiating two conditions which are normally difficult to identify. These two conditions are ureteral obstruction and renal vein occlusion. Clinically, this could be very helpful in screening patients with renal problems. The flow index is also abnormal when acute renal failure is present. However, since some of the conditions induced in this research were extreme conditions, we feel that further studies should be done investigating such conditions as partial ureteral obstruction and partial renal vein occlusion. These studies would help to identify the limitations of the flow index and are planned in further research.

One of the abnormalities studied in this research, renal artery stenosis, was not predicted precisely by the model. However, the stenosis induced was moderate which makes detection difficult. Therefore, further study using more severe degrees of stenosis is also planned in further research.

Finally, in the future, we hope to use this model in a clinical nuclear medicine department to aid clinicians in diagnosing renal disease.

BIBLIOGRAPHY

1. BAUER, J. D., P. G. ACKERMANN and G. TORO. Bray's Clinical Laboratory Methods. 7th ed., St. Louis, C. V. Mosby Company, 1968, pp. 58-66.
2. BAUMAN, J. W. and F. P. CHINARD. Renal Function. St. Louis, C. V. Mosby Company, 1975, pp. 40-45.
3. BAUMAN, J. W. and F. P. CHINARD. Renal Function. St. Louis, C. V. Mosby Company, 1975, pp. 64-66.
4. BLAUFox, M. D. (vol. editor). Progress in Nuclear Medicine, Vol. 2, Evaluation of Renal Function and Disease with Radionuclides. Baltimore, University Park Press, 1972, pp. 21, 54-67.
5. BLAUFox, M. D. (vol. Editor). Progress in Nuclear Medicine, Vol. 2, Evaluation of Renal Function and Disease with Radionuclides. Baltimore, University Park Press, 1972, p. 255.
6. BLAUFox, M. D., H. G. FROHMULLER, J. C. CAMPBELL, D. C. UTZ, A. L. ORVIS and C. A. OWEN. A simplified method of estimating renal function with iodohippurate I-131. J. Surg. Res. 3:122-125, 1963.
7. BLAUFox, M. D. and J. P. MERRILL. Compartmental analysis of the hippuran I-131 renogram in man. Fed. Proc. 24:405, 1965.
8. BLAUFox, M. D. and J. P. MERRILL. Measurement of renal function in man with simplified hippuran clearances. Nephron 3:274-279, 1966.
9. BLAUFox, M. D. and J. P. MERRILL. Evaluation of renal transplant function by iodohippurate sodium I-131. JAMA 202:575-578, 1967.
10. BLAUFox, M. D., A. L. ORVIS and C. A. OWEN. Compartment analysis of the radiorenogram and distribution of hippuran I-131 in dogs. Amer. J. Physiol. 204:1059-1064, 1963.
11. BLAUFox, M. D., E. J. POTCHEN and J. P. MERRILL. Measurement of effective renal plasma flow in man by external counting methods. J. Nucl. Med. 8:77-85, 1967.
12. BRITTON, K. E. and J. G. BROWN. The clinical use of C.A.B.B.S. renography. Br. J. Radiol. 41:570-579, 1968.
13. BURBANKE, M. K., W. N. TAUXE and F. T. MAHER. Evaluation of radioiodinated hippuran for the estimation of renal plasma flow. Proc. Staff Meet. Mayo Clin. 36:372-386, 1961.
14. CHISHOLM, G. D., K. EVANS and A. E. KULATILAKE. The quantitation of renal blood flow using I-125 hippuran. Brit. J. of Urol. 39:50-57, 1967.

15. CHISHOLM, G. D., M. D. SHORT and H. I. GLASS. The measurement of individual renal plasma flows using I-123 hippuran and the gamma camera. *Brit. J. Urol.* 46:591-600, 1974.
16. CUTLER, R. E. and H. GLATTE. Simultaneous measurement of glomerular filtration rate and effective renal plasma flow with Co-57 cyanocobalamin and I-125 hippuran. *J. Lab. Clin. Med.* 65:1041-1046, 1965.
17. DABAJ, E., H. MENGES and W. H. PRITCHARD. Determination of renal blood flow by single injection of hippuran I-131 in man. *Am. Heart Journal*, 71:79-83, 1966.
18. D'ARGENIO, D. Z. and A. SCHUMITZKY. A program package for simulation and parameter estimation in pharmacokinetic systems. *Computer Programs in Biomed.* 9:115-134, 1979.
19. DeGRAZIA, J. A., P. O. SCHEIBE, P. E. JACKSON, Z. J. LUCAS, W. FAIR, J. VOGEL and L. BLUMIN. Clinical applications of a kinetic model of hippurate distribution and renal clearance. *J. Nucl. Med.* 15:102-114, 1974.
20. EARLEY, L. and C. GOTTSCHALK (editors). *Strauss and Welt's Diseases of the Kidney*, Vol. II. 3rd ed., Boston, Little, Brown and Company, 1979, pp. 1371-1394.
21. EARLY, P. and D. SODEE. *Technology and Interpretation of Nuclear Medicine Procedures*. 2nd ed., St. Louis, C. V. Mosby Company, 1975, pp. 208-209.
22. FLAMENBAUM, W. J. S. MCNEILL, T. A. KOTCHEN and A. J. SALADINO. Experimental acute renal failure induced by uranyl nitrate in the dog. *Circ. Res.* 31:682-697, 1972.
23. FARMELANT, M. H. A region of interest system to reduce tissue background in renograms. *J. Nucl. Med.* 11:267, 1970.
24. FARMER, C. D., W. N. TAUXE, F. T. MAHER and J. C. HUNT. Measurement of renal function with radioiodinated diatrizoate and o-iodohippurate. *Amer. J. Clin. Path.* 47:9-16, 1967.
25. GAGNON, J. A. and L. U. MAILLOUX. Differences in simultaneous and sequential clearances of I-131-iodohippurate and p-aminohippurate. *Amer. Soc. Nephrol.* 1:21, 1967.
26. GAGNON, J. A., L. U. MAILLOUX, J. E. DOOLITTLE and P. E. TESCHAN. An isotopic method for instantaneous measurements of effective renal blood flow. *Amer. J. Physiol.* 218:180-186, 1970.
27. GOTT, F. S., W. H. PRITCHARD, W. R. YOUNG and W. J. MAC INTYRE. Renal blood flow measurement from the disappearance of intravenously injected hippuran. *J. Nucl. Med.* 3:480-485, 1962.

28. GUYTON, A. C. Textbook of Medical Physiology. 5th ed., Philadelphia, W. B. Saunders Company, 1976, pp. 438-440.
29. HOLROYD, A. M., G. D. CHISHOLM and H. I. GLASS. The quantitative analysis of renograms using the gamma camera. *Phys. Med. Biol.* 15:483-492, 1970.
30. HOLROYD, A. M. and T. JONES. A simple method for obtaining dynamic quantitative information from the gamma camera. *Phys. Med. Biol.* 14:631-638, 1969.
31. HAYES, M., S. BROSMAN and G. V. TAPLIN. Determination of differential renal function by sequential renal scintigraphy. *J. of Urol.* 111:556-559, 1974.
32. MAGNUSSON, G. A. Kidney function studies with I-131 tagged sodium orthohippurate. *Acta. Med. Scand. [Suppl]* 171:94-124, 1962.
33. MAHER, F. T. and W. N. TAUXE. Renal clearance in man of pharmaceuticals containing radioactive iodine, Influence of plasma binding. *JAMA* 207:97-104, 1969.
34. MATTHEWS, C. M. The theory of tracer experiments with I-131 labeled plasma proteins. *Physics Med. Bio.* 2:36-53, 1957.
35. MESCHAN, I., H. E. SCHMID, F. C. WATTS and R. WITCOFSKI. The utilization of radioactive iodinated hippuran for determination of renal clearance rates. *Radiology* 81:437-446, 1963.
36. MITTA, A. E., A. FRAGA and N. VEALL. A simplified method for preparing I-131 labeled hippuran. *Int. J. Appl. Radiat. Isotopes* 12:146-147.
37. NELOER, J. and R. MEAD. A simple method for function minimization. *Comput. J.* 4:308-313, 1965.
38. NORMAN, N. Effective plasma flow of the individual kidney. Determination on the basis of the I-131 hippuran renogram. *Scand. J. Clin. Lab. Invest.* 30:395-403, 1972.
39. OLSSON, D. and L. NELSON. The Nelder-Mead simplex procedure for function minimization. *Technometrics* 17:45-51, 1975.
40. PITTS, R. F. *Physiology of the Kidney and Body Fluids.* 3rd ed. Chicago, Year Book Medical Publishers, Inc., 1974, pp. 1-8.
41. PITTS, R. F. *Physiology of the Kidney and Body Fluids.* 3rd ed. Chicago, Year Book Medical Publishers, Inc., 1974, pp. 158-161.

42. PRITCHARD, W. H., R. W. ECKSTEIN, W. J. MAC INTYRE and E. DABAJ. Correlation of renal blood flow determined by the single injection of hippuran I-131 with direct measurements of flow. *Am. Heart Journal* 70:789-796, 1965.
43. RAM, M. D., K. EVANS and G. D. CHISHOLM. Measurement of effective renal plasma flow by the clearance of I-125 hippuran. *Lancet* 645-646, 1967.
44. RAM, M. D., K. EVANS AND G. D. CHISHOLM. A single injection method for measurement of effective renal plasma flow. *Brit. J. Urol.* 40:425-428, 1968.
45. SAPIRSTEIN, L. A., D. G. VIDT, M. J. MANDEL and G. HANUSEK. Volumes of distribution and clearances of intravenously injected creatinine in the dog. *Am. J. Physiol.* 181:330-336, 1955.
46. SCHLEGEL, J. U. and B. T. BAKULE. A diagnostic approach in detecting renal and urinary tract disease. *J. Urol.* 104:2-10, 1970.
47. SCHLEGEL, J. U., B. G. SMITH and R. M. O'DELL. Estimation of effective renal plasma flow using I-131 labeled hippuran. *J. Appl. Physiol.* 17:80-82, 1962.
48. SCHWARTZ, F. D. and M. S. MADELHOFF. Simultaneous renal clearances of radiohippuran and PAH in man. *Clin. Res.* 9:208, 1961.
49. SCHWARTZ, F. D. and M. S. MADELHOFF. Use of radio-hippuran in diagnosis of unilateral renal disease. *J. Urol.* 87:244-257, 1961.
50. SHAMPINE, L. and M. GORDON. *Computer Solution of Ordinary Differential Equations.* San Francisco, W. H. Freeman, 1975.
51. SHORT, M. D., H. I. GLASS, G. D. CHISHOLM, P. VERNON and D. J. SILVESTER. Gamma camera renography using I-123 hippuran. *Brit. J. Radiol.* 46:289-294, 1973.
52. SMITH, H. W. *Principals of Renal Physiology.* New York, Oxford University Press, 1956, p. 32.
53. SMITH, H. W. *Principals of Renal Physiology.* New York, Oxford University Press, 1956, p. 58.
54. SMITH, H. W. *Principals of Renal Physiology.* New York, Oxford University Press, 1956, p. 200.
55. SMITH, H. W., N. FINKLESTEIN and L. ALIMINOSA. The renal clearances of substituted hippuric acid derivative and other aromatic acids in the dog and man. *J. Clin. Invest.* 24:388-404, 1945.

56. STADALNICK, R. C., J. M. VOGEL, A. JANSOLT, K. A. KROHN, N. M. MATOLO, M. LAGUNAS-SOLAR and F. ZIELINSKI. Renal clearance and extraction parameters of ortho-iodohippurate (I-123) compared with OIH (I-131) and PAH. *J. Nucl. Med.* 21:168-170, 1980.
57. STOKES, J. M. and M. M. TER-POGOSSIAN. Double isotope technique to measure renal functions. *JAMA* 187:20-23, 1964.
58. SUMMERS, R. E., J. P. CONCANNON, C. WEILS and C. COLE. Determination of simultaneous effective renal plasma flow and glomerular filtration rate with I-131-o-iodohippurate and I-125-allyl inulin. *J. Lab. Clin. Med.* 69:919-926, 1967.
59. TAPLIN, G. V., E. K. DORE and D. E. JOHNSON. The quantitative radiorenogram for total and differential renal blood flow measurements. *J. Nucl. Med.* 4:404-409, 1963.
60. TAPLIN, G. V., O. M. MERIDITH, H. KADE and C. C. WINTER. The radioisotope renogram. *J. Lab. Clin. Med.* 48:886-901, 1956.
61. TAUXE, W. N. and J. C. HUNT. Evaluation of renal function by isotope techniques. *Medical Clinics of North America* 50:937-954, 1966.
62. TAUXE, W. N., F. T. MAHER and W. F. TAYLOR. Effective renal plasma flow: Estimation from theoretical volumes of distribution of intravenously injected I-131 orthoiodohippurate. *Mayo Clin. Proc.* 46:524-531, 1971.
63. TUBIS, M., E. POSNICK and R. A. NORDYKE. Preparation and use of I-131 kidney labeled sodium iodohippurate in kidney function tests. *Proc. Soc. Exp. Biol. Med.* 103:497-498, 1960.
64. VANDER, A. J. *Renal Physiology*. New York, McGraw-Hill Book Company, 1975, pp. 4-12.
65. VANDER, A. J. *Renal Physiology*. New York, McGraw-Hill Book Company, 1975, p. 30.
66. VISBAL, GEOFFREY (Chief Technologist for Cardiology Research Group, Loma Linda University Hospital). Personal Communication.
67. WAGONER, R. D., W. N. TAUXE and F. T. MAHER. Measurement of effective renal plasma flow with sodium iodohippurate I-131. *JAMA* 187:811-813, 1964.
68. WELLER, J. M. (editor). *Fundamentals of Nephrology*. New York, Harper and Row, 1979, p. 189.
69. WITCOFSKI, R. L., J. E. WHITLEY, I. MESCHAN and W. E. PAINTER. A method and parameters for the analysis of renal function by external scintillation detector technic. *Radiology* 76:621-627, 1961.